Direct determination of the strange and light quark condensates from full lattice QCD

C. McNeile,[1,*] A. Bazavov,[2] C. T. H. Davies,[3,†] R. J. Dowdall,[3] K. Hornbostel,[4] G. P. Lepage,[5] and H. D. Trottier[6,7]

[1]*Bergische Universität Wuppertal, Gaussstrasse 20, D-42119 Wuppertal, Germany*
[2]*Physics Department, Brookhaven National Laboratory, Upton, New York 11973, USA*
[3]*School of Physics and Astronomy, SUPA, University of Glasgow, Glasgow G12 8QQ, United Kingdom*
[4]*Southern Methodist University, Dallas, Texas 75275, USA*
[5]*Laboratory of Elementary-Particle Physics, Cornell University, Ithaca, New York 14853, USA*
[6]*Physics Department, Simon Fraser University, 8888 University Drive, Burnaby, British Columbia V5A 1S6, Canada*
[7]*TRIUMF, 4004 Westbrook Mall, Vancouver, British Columbia V6T 2A3, Canada*

We determine the strange quark condensate from lattice QCD for the first time and compare its value to that of the light quark and chiral condensates. The results come from a direct calculation of the expectation value of the trace of the quark propagator followed by subtraction of the appropriate perturbative contribution, derived here, to convert the non-normal-ordered $m\bar{\psi}\psi$ to the $\overline{\text{MS}}$ scheme at a fixed scale. This is then a well-defined physical ''nonperturbative'' condensate that can be used in the operator product expansion of current-current correlators. The perturbative subtraction is calculated through $\mathcal{O}(\alpha_s)$ and estimates of higher order terms are included through fitting results at multiple lattice spacing values. The gluon field configurations used are ''second generation'' ensembles from the MILC collaboration that include $2 + 1 + 1$ flavors of sea quarks implemented with the highly improved staggered quark action and including u/d sea quarks down to physical masses. Our results are $\langle \bar{s}s \rangle^{\overline{\text{MS}}}(2 \text{ GeV}) = -(290(15) \text{ MeV})^3$, $\langle \bar{l}l \rangle^{\overline{\text{MS}}}(2 \text{ GeV}) = -(283(2) \text{ MeV})^3$, where l is a light quark with mass equal to the average of the u and d quarks. The strange to light quark condensate ratio is 1.08 (16). The light quark condensate is significantly larger than the chiral condensate in line with expectations from chiral analyses. We discuss the implications of these results for other calculations.

I. INTRODUCTION

A critical feature of the nonperturbative dynamics of QCD at zero temperature is the condensation of quark-antiquark pairs in the vacuum, spontaneously breaking the chiral symmetry of the action. The value of the chiral condensate (the quark condensate at zero quark mass) is then an important parameter for low-energy QCD [1]. The well-known Gell-Mann-Oakes-Renner (GMOR) relation [2]

$$\frac{f_\pi^2 M_\pi^2}{4} = -\frac{m_u + m_d}{2} \frac{\langle 0|\bar{u}u + \bar{d}d|0\rangle}{2} \quad (1)$$

connects the u/d quark masses times the condensate to the square of the mass times the decay constant for the Goldstone boson of the spontaneously broken symmetry. Equation (1) has normalization such that $f_\pi = 130$ MeV. The GMOR relation holds in the limit of m_u, $m_d \rightarrow 0$. A value for this chiral condensate can be derived from the chiral extrapolation of lattice QCD results for light meson masses and decay constants. See, for example, the recent result of $-(272(2) \text{ MeV})^3$ for the chiral condensate in the $\overline{\text{MS}}$ scheme at 2 GeV using SU(2) chiral perturbation theory [3].

The determination of the quark condensate for nonzero quark masses is more problematic because, depending on

the method used, there are various sources of unphysical quark mass dependence and a careful definition of the condensate is required. This definition must be phrased in terms of the operator product expansion (OPE) since this is the context in which the condensate appears [1,4,5]. The OPE allows us to separate short- and long-distance contributions in, for example, a short-distance current-current correlator. The expansion is in terms of a set of matrix elements of local operators multiplied by coefficient functions. The aim is for all the long-distance contributions (with scale $< \mu$) to be contained in the matrix elements and the short distance contributions (with scale $> \mu$) in the coefficient functions. A key matrix element, since it corresponds to a relatively low-dimensional ($d = 3$) operator, is that of the quark condensate. The clean separation of scales in the OPE only works if the local operators are *not* normal ordered [6,7]. Then the coefficient functions are analytic in the quark masses and therefore free of infrared sensitivity. This means, however, that the quark mass dependent mixing of $m\bar{\psi}\psi$ with the unit operator must be taken into account and that the vacuum matrix element of $m\bar{\psi}\psi$ is not cutoff independent. The quantity that appears in the OPE is the vacuum matrix element in, for example, the $\overline{\text{MS}}$ scheme at the scale μ. We can derive this matrix element from lattice QCD and we give results here for $\mu = 2$ GeV. The results can easily be run to other scales, as appropriate.

*mcneile@uni-wuppertal.de
†c.davies@physics.gla.ac.uk

The value of the condensate for quarks of nonzero mass up to that of the strange quark is needed in a number of calculations involving light quark correlators. In lattice QCD it is frequently easier and statistically more precise to use strange quarks than very light quarks in contexts where the quark mass is not expected to be important. Then the strange quark condensate appears in the calculation, however. Examples include the matching to continuum QCD perturbation theory of lattice QCD calculations of moments of heavy-light meson correlators [8] and of light meson correlators at large spacelike q^2 [9]. Such calculations are used to extract quark masses and the strong coupling constant, α_s. A continuum example where the strange quark condensate is needed is in the determination of the strange quark mass, m_s, from hadronic τ decays [10].

Current estimates of the value of the strange quark condensate vary by almost a factor of 2 [11,12]. It is not even clear whether the strange condensate is larger or smaller than the light quark condensate. For very large quark masses, $m_q > \Lambda_{\text{QCD}}$, say, so that the quark mass dominates the propagator, it seems clear that the condensate should fall to zero, but this does not help in determining the slope of the condensate with m_q for small quark masses.

Here we address the determination of the strange (or other nonzero mass) quark condensate by direct calculation in full lattice QCD. By direct we mean that we determine the vacuum expectation value of the strange quark propagator as well as the light quark propagator on a range of gluon field configurations at different values of the lattice spacing and sea quark masses. To isolate the low-energy nonperturbative value of the condensate from these results requires the subtraction of a perturbative contribution. The perturbative contribution in lattice QCD has two pieces. One diverges as $a \rightarrow 0$ and dominates the vacuum expectation value of the strange quark propagator, particularly on our finer lattices. The second piece contains infrared sensitive logarithms of the quark mass which cancel against similar terms in continuum perturbation theory allowing an infrared safe definition of the condensate for use in the OPE, as discussed above.

The error in the final result then depends on how well this subtraction can be done. Here we use an explicit calculation of the perturbative pieces through $\mathcal{O}(\alpha_s)$ and fit for unknown higher order terms. The known quark mass and a dependence of these unknown terms help in constraining them along with the very small statistical errors in our lattice results. We also use a particularly good discretization of the Dirac action known as the highly improved staggered quark (HISQ) formalism [13] on second generation gluon field configurations so that discretization errors in the physical nonperturbative results are small.

The paper is laid out as follows. In Sec. II we describe the theoretical background to direct calculations of the quark condensate in lattice QCD. Section III gives our

lattice QCD results on gluon configurations with $2 + 1 + 1$ flavors of sea quarks, describing the calculation of the perturbative contribution that is subtracted and then the procedure for fitting the remaining nonperturbative condensates as a function of quark mass and lattice spacing. We also give results from configurations including $2 + 1$ flavors of sea quarks over a wider range of lattice spacing values but studying only the strange quark condensate in Appendix D. In Sec. IV we compare to previous values and discuss the implications of our results for both zero and finite temperature QCD calculations. Section V gives our conclusions.

II. THEORETICAL BACKGROUND

The direct determination of the chiral condensate in lattice QCD requires the calculation of the expectation value over an ensemble of gluon fields, U, of $\text{Tr}M^{-1}$ where M is the lattice discretization of the Dirac matrix. The quark action for a given quark flavor,

$$S_f = \bar{\psi} M_f \psi \tag{2}$$

and

$$\langle \bar{\psi}\psi \rangle = \langle 0|\bar{\psi}_f \psi_f|0\rangle = -\frac{1}{V}\langle \text{Tr}M_f(U)^{-1}\rangle_U, \tag{3}$$

where the trace is over spin, color and space-time point and the gluon fields in the ensemble used for the average include the effect of sea quarks (of all flavors, not just f) in their probability distribution. V is the lattice volume, $L^3 \times T$. For a naive discretization of the Dirac action M takes the form

$$M = \gamma_\mu \Delta_\mu + m, \tag{4}$$

where Δ_μ is a covariant finite difference on the lattice

$$\Delta_\mu \psi_x = \frac{1}{2a}(U_\mu(x)\psi(x+\hat{\mu}) - U_\mu^\dagger(x-\hat{\mu})\psi(x-\hat{\mu})) \tag{5}$$

and m is the quark mass for that flavor. Because of fermion doubling this formalism describes 16 "tastes" of quarks in four dimensions rather than just one and we must divide the right-hand side of Eq. (3) by the number of tastes, $N_t = 16$. The staggered formalism is derived from this naive formalism by a rotation which allows the spin degree of freedom to be dropped. In that case the quark field becomes a one-component spinor, which is numerically very efficient, and $N_t = 4$.

For $m = 0$ the eigenvalues of M for either naive or staggered quarks are purely imaginary and come in $\pm$ pairs. Therefore, in the absence of exact zero modes,

$$-\langle \bar{\psi}\psi \rangle = \frac{1}{N_t}\sum_\lambda \left(\frac{1}{m+i\lambda} + \frac{1}{m-i\lambda}\right) = \frac{1}{N_t}\sum_\lambda \frac{2m}{m^2+\lambda^2}. \tag{6}$$

A calculation at $m = 0$ on a finite volume lattice would then give an answer for the quark condensate of zero.

This does not mean that chiral symmetry is unbroken, however. The problem arises because the broad distribution of nonzero eigenvalues (ignoring topological near-zero modes) drops to zero near the origin in a way that depends strongly on the volume. Once the quark mass is below the minimum of the nonzero eigenvalues the result for $\langle \bar{\psi} \psi \rangle$ will be distorted. A more careful consideration of limits must be made. If V is taken to infinity before m is taken to zero then the sum over eigenvalues can be replaced by an integral and the Banks-Casher relation [14] is obtained. This connects the zero-mass condensate to the spectral density at the origin:

$$\Sigma = -\langle \bar{\psi} \psi (m = 0) \rangle = \frac{\pi \rho(0)}{N_t}. \quad (7)$$

Thus Σ can be obtained from studies of the spectral density and, more recently, has also been obtained from matching the distribution of low eigenmodes to random matrix theory in the ϵ regime [15–17]. Here we are more concerned with extracting a condensate at nonzero quark mass, for example at the strange quark mass, and so the issue above is not relevant. We will work on large volume lattices (over ten times larger than the study in Ref. [18] that looked at staggered eigenvalues in the ϵ regime) at quark mass values that are well within the distribution of nonzero eigenvalues. Our results for $\langle \mathrm{Tr} M^{-1} \rangle$ then include both the effects of a nonzero value for $\rho(0)$ and a nonzero quark mass.

A second issue arises, however, in the extraction of a physical nonperturbative value for the condensate at nonzero quark mass. A perturbative contribution appears from mixing between the scalar $\bar{\psi} \psi$ operator and the identity since the identity operator has a vacuum expectation value in the trivial perturbative vacuum. This perturbative contribution vanishes at zero quark mass since chiral symmetry is not broken in perturbation theory [for the same reason as that given on the lattice above in Eq. (6)]. At nonzero quark mass it contains odd powers of m starting with a quadratically ultraviolet divergent term linear in m. This can be illustrated with a tree-level calculation in the continuum to give

$$-\langle \bar{\psi} \psi \rangle = \int_0^\Lambda \frac{d^4 k}{(2\pi)^4} \frac{12m}{k^2 + m^2} = \frac{3}{4\pi^2} \left(m\Lambda^2 + m^3 \log \frac{m^2}{\Lambda^2 + m^2} \right). \quad (8)$$

The quadratic ultraviolet divergence depends on the scheme used but the $m^3 \log(m/\Lambda)$ term is universal since it arises from the infrared part of the integral. The coefficient above agrees with that obtained for the $\overline{\mathrm{MS}}$ scheme in Ref. [19] and on the lattice for highly improved staggered quarks to be described in Sec. III A. We stress that a perturbative contribution of this kind is present for all lattice regularizations of QCD, whatever their chiral symmetry properties, and so must be calculated and subtracted to give a physical result. The quadratic divergence present for Ginsparg-Wilson fermions is demonstrated in the

quenched approximation in, for example, Ref. [20] and the additional divergences for the Wilson formalism with broken chiral symmetry in Ref. [21].

This subtraction is somewhat analogous to subtracting perturbative contributions to the mean plaquette to obtain the nonperturbative gluon condensate. That, however, is extremely difficult to do because the nonperturbative condensate contribution to the plaquette is so small. This contribution is given at leading order by

$$\delta P_{\mathrm{cond}} = -\frac{\pi^2}{36} a^4 \langle \alpha_s G^2 / \pi \rangle. \quad (9)$$

If we take the value of the gluon condensate as $\mathcal{O}(\Lambda_{\mathrm{QCD}}^4)$ then $\langle \alpha_s G^2 / \pi \rangle \approx 0.005 \ \mathrm{GeV}^4$. On very coarse lattices for which $a \approx 1 \ \mathrm{GeV}^{-1}$, this contributes less than 1% to the value of the plaquette. On finer lattices the nonperturbative condensate contribution is even smaller because it falls as a^4 while the perturbative contribution falls only as $\alpha_s(d/a)$ for some scale d. This means that the plaquette is in fact a very good variable to use for the determination of α_s from lattice QCD calculations but not for the determination of the gluon condensate [22]. For larger Wilson loops the gluon condensate contribution is larger, being proportional to the square of the area of the loop, but the coefficients in the perturbative series also become larger.

The determination of the nonperturbative quark condensate from $\langle \mathrm{Tr} M^{-1} \rangle$ is in much better shape than this for several reasons. The main one is that the nonperturbative condensate contribution to $\langle \mathrm{Tr} M^{-1} \rangle$ in lattice units is only a factor of a^2 smaller than the leading perturbative contribution rather than a^4. In addition the perturbative contribution is suppressed by the quark mass, which is small for the u/d and s quarks we will consider here. The perturbative contribution is a well-defined function of the quark mass at every order in perturbation theory and so results at several values of the quark mass, and the lattice spacing, can be used to constrain unknown higher orders, beyond the $\mathcal{O}(\alpha_s)$ that we have explicitly calculated, and we will make use of that here.

III. LATTICE QCD CALCULATION ON $n_f = 2 + 1 + 1$ GLUON CONFIGURATIONS

The gluon field configurations used here are listed in Table I. They were generated by the MILC collaboration [24] using a tadpole-improved Lüscher-Weisz gauge action with coefficients corrected perturbatively through $\mathcal{O}(\alpha_s)$ including pieces proportional to n_f, the number of quark flavors in the sea [25]. The gauge action is then improved completely through $\mathcal{O}(\alpha_s a^2)$. Sea quarks are included with the HISQ action [13] which has been designed to have very small discretization errors. Discretization errors are formally removed through $\mathcal{O}(a^2)$ but higher order errors, particularly staggered taste-changing errors, are seen to be smaller with HISQ than with the earlier asqtad staggered quark action [13,24]. The HISQ action used here has

TABLE I.   Details of the MILC gluon field ensembles used in this paper. $\beta = 10/g^2$ is the $SU(3)$ gauge coupling and L/a and T/a are the number of lattice spacings in the space and time directions for each lattice. $am_{l,\text{sea}}$, $am_{s,\text{sea}}$ and $am_{c,\text{sea}}$ are the light (up and down taken to have the same mass), strange and charm sea quark masses in lattice units. a is the lattice spacing in fm determined from the decay constant of the η_s meson in Ref. [23] with values for 3, 6 and 8 added here. The ensembles 1, 2 and 3 will be referred to in the text as "very coarse," 4, 5 and 6 as "coarse" and 7 and 8 as "fine."

Set	β	a/fm	$am_{l,\text{sea}}$	$am_{s,\text{sea}}$	$am_{c,\text{sea}}$	$L/a \times T/a$
1	5.80	0.1546(11)	0.013	0.065	0.838	16×48
2	5.80	0.1526(8)	0.0064	0.064	0.828	24×48
3	5.80	0.1511(8)	0.00235	0.0647	0.831	32×48
4	6.00	0.1234(8)	0.0102	0.0509	0.635	24×64
5	6.00	0.1218(6)	0.00507	0.0507	0.628	32×64
6	6.00	0.1206(6)	0.00184	0.0507	0.628	48×64
7	6.30	0.0899(7)	0.0074	0.0370	0.440	32×96
8	6.30	0.0875(7)	0.0012	0.0363	0.432	64×96

two smearing steps for the gluon field appearing in the quark action with a U(3) projection of the smeared links between the two smearing steps. The configurations include a sea charm quark in addition to up, down and strange. These configurations are then said to have $2 + 1 + 1$ flavors in the sea, since the u and d quarks are taken to have the same mass (denoted m_l here). This is heavier than the average u/d mass in the real world on most of the configuration sets but there are three for which the u/d mass has its physical value (3, 6 and 8). The s and c masses are tuned as closely as possible to their correct values on each set. The tuning of the sea s quark mass is accurately done—typically to better than 5%—so the u/d quark mass can be accurately calibrated in terms of the s quark mass for chiral extrapolations.

The s quark mass is tuned using a pseudoscalar bound state of an s quark-antiquark pair known as the η_s. Because we do not include disconnected diagrams in the η_s correlators it is unable to decay to gluons or to mix with the physical η and η' mesons. However, its properties can be accurately determined in lattice QCD in the continuum and chiral limits from the physical properties of the π and K [26]. We then use the η_s decay constant to determine the lattice spacing and this was done for most ensembles in Table 1 in Ref. [23]. The values vary from 0.15 to 0.09 fm as we go from the very coarse to the fine lattices. The spatial volumes are large, from $(2.5 \text{ fm})^3$ when $m_l/m_s \approx 0.2$ to $(3.7 \text{ fm})^3$ when $m_l/m_s \approx 0.1$.

On each of these ensembles we determine $\langle \text{Tr} M^{-1} \rangle$ for HISQ valence quarks for various quark masses. To do this we use an identity that relates the quark propagator for staggered quarks to a product of quark propagators:

$$\frac{1}{am_q} \text{Tr} M_{00}^{-1} = \sum_n \text{Tr}[M_{0n}^{-1} M_{n0}^{-1}](-1)^n = \sum_n \text{Tr}|M_{0n}^{-1}|^2. \quad (10)$$

Here 0 and n are arbitrary lattice sites and am_q is the quark mass in lattice units used for the quark propagator. The right-hand side of Eq. (10) is simply the correlator between 0 and n for the Goldstone pseudoscalar meson made of a

quark and antiquark of mass am_q. Summing over n projects on to zero spatial momentum and sums over time slices. Thus, dividing both sides by 4, the number of tastes for staggered quarks, we obtain

$$-a^3 \langle \bar{\psi} \psi \rangle_0 = (am_q) \sum_t C_\pi(t). \quad (11)$$

The raw condensate value on the left-hand side of this expression is normalized to the single flavor case and the pion correlator on the right-hand side is the usual zero-momentum Goldstone meson correlator. This allows us to determine $\langle \bar{\psi} \psi \rangle_0$ by summing over the Goldstone pseudoscalar correlators calculated in Ref. [23]. Equation (10) is derived in Ref. [27] for a single propagator origin, 0, but the derivation can trivially be extended to hold for the random wall source that we use for our correlators in Ref. [23]. The identity holds configuration by configuration for lattice QCD quark formalisms with sufficient chiral symmetry and in the continuum for a specific gauge field background. We give an explicit proof of this in Appendix A. Since our Goldstone pseudoscalar correlators are sums of positive numbers they are particularly precise and this precision then carries over to our condensate results. For the light condensate we use the pion correlators made of light quarks and for the strange condensate we use the η_s correlators made of strange quarks. We stress that what we calculate using Eq. (10) is the vacuum expectation value of the condensate (and not a specific "in-meson" value) despite the fact that we determine it for convenience from a meson correlator.

Table II gives the valence quark masses used in our calculation and the raw results for the condensate obtained from Eq. (10). The correlator calculations used 16 "random wall" time sources on approximately one thousand configurations in each ensemble (somewhat fewer on sets 6 and 8) and so the results have very small statistical errors. The valence light quark masses are equal to those in sea (except for a very small change on set 3) but we have shifted the valence strange quark masses slightly to be

TABLE II.　Raw (unsubtracted) values for the light and strange quark condensates in lattice units calculated for valence masses given in columns 2 and 3. The results use the correlators calculated in Ref. [23] [via Eq. (11)], but we also give results for additional strange quark masses on sets 1 and 2 and new results on sets 3, 6 and 8. We have 16,000 correlators per ensemble, except for sets 6 and 8 where we use approximately 10000.

Set	$am_{l,\text{val}}$	aM_π	af_π	$-a^3\langle\bar{\psi}\psi_l\rangle_0$	$am_{s,\text{val}}$	aM_{η_s}	af_{η_s}	$-a^3\langle\bar{\psi}\psi_s\rangle_0$
1	0.013	0.23637(15)	0.11183(9)	0.018607(29)	0.0688	0.53361(14)	0.14199(6)	0.045758(19)
					0.0641	0.51491(14)	0.13996(6)	0.043616(19)
2	0.0064	0.16615(7)	0.10511(5)	0.014524(18)	0.0679	0.52797(8)	0.14026(3)	0.045009(12)
					0.0636	0.51078(8)	0.13839(3)	0.043038(12)
3	0.00235	0.10172(5)	0.09934(5)	0.011762(11)	0.0628	0.50657(5)	0.13720(3)	0.042483(6)
4	0.01044	0.19153(9)	0.09075(5)	0.011629(13)	0.0522	0.42351(9)	0.11312(4)	0.031756(10)
5	0.00507	0.13413(5)	0.08451(4)	0.008511(9)	0.0505	0.41476(6)	0.11119(2)	0.030768(6)
6	0.00184	0.08154(2)	0.07988(2)	0.006534(6)	0.0507	0.41481(2)	0.11062(2)	0.030768(4)
7	0.0074	0.14070(9)	0.06621(5)	0.006153(8)	0.0364	0.30884(11)	0.08238(4)	0.019822(4)
8	0.0012	0.05718(2)	0.05781(3)	0.002803(4)	0.0360	0.30483(4)	0.08055(2)	0.019504(2)

closer to the physical strange quark mass, following Ref. [23]. On sets 1 and 2 we give results for two different values of the strange quark mass, to help in constraining the valence mass dependence of the condensate.

Errors on the condensate values are determined after binning over adjacent sets of at least five configurations, following analysis of the autocorrelation function. An example plot is shown, for coarse set 6, in Fig. 1. The autocorrelation function is defined as

$$C_{\Delta T} = \frac{\langle x_i x_{i+\Delta T}\rangle - \langle x_i\rangle\langle x_{i+\Delta T}\rangle}{\langle x_i^2\rangle - \langle x_i\rangle^2}. \tag{12}$$

Here x_i represents a condensate value on configuration i and $x_{i+\Delta T}$ that on a configuration a further ΔT time units along in the ordered ensemble. $\Delta T = 1$ thus corresponds to
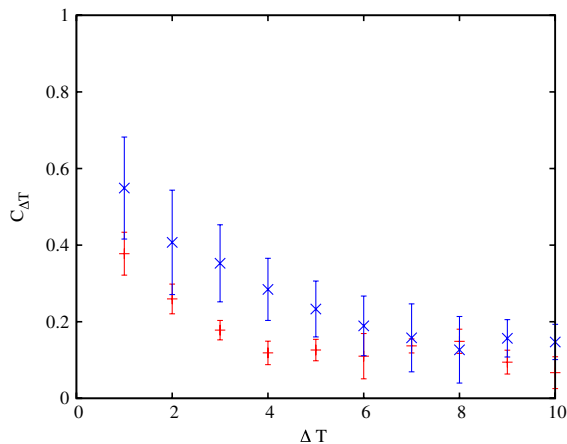

FIG. 1 (color online). Autocorrelation function, $C_{\Delta T}$ of Eq. (12), for the strange and light quark condensates on coarse set 6 with physical mass light sea quarks. The x axis, ΔT, is the separation in time units between configurations. The strange condensate results are given as blue crosses and the light condensate with red pluses. Errors in $C_{\Delta T}$ are estimated by dividing the configuration time series into five consecutive sets.

adjacent configurations. Figure 1 shows that nearby configurations in the ensembles are correlated and thus binning is necessary to obtain a reliable statistical error. A similar analysis applies to masses and decay constants as discussed in Ref. [23].

In the next section we describe the perturbative calculation of the condensate which we will then subtract from the raw results of Table II to enable the nonperturbative condensate to be determined.

A. Perturbative calculation of $\langle\text{Tr}M^{-1}\rangle$

We computed the perturbative contribution $\langle\bar{\psi}\psi\rangle_{\text{PT}}$ to the chiral condensate for the HISQ action through first order in α_s:

$$-a^3\langle\bar{\psi}\psi\rangle_{\text{PT,HISQ}} = am_0 \times [c_0(am_0) + c_1(am_0)\alpha_s + O(\alpha_s^2)], \tag{13}$$

where am_0 is the bare quark mass parameter that appears in the HISQ action. The Feynman diagrams required for this order are shown in Fig. 2. The perturbative quadratic ultraviolet divergence discussed in Eq. (9) shows up as finite values for the perturbative coefficients, as defined above, in the limit $am_0 \to 0$.

We computed the coefficients from numerical evaluation of the lattice loop integrals over a range of masses that includes the light and strange quark masses that we have
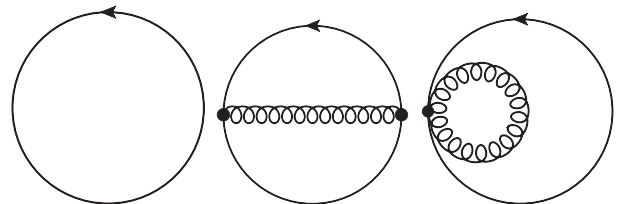

FIG. 2.　Feynman diagrams for the calculation of the perturbative contribution to the quark condensate through $\mathcal{O}(\alpha_s)$.

TABLE III. Zeroth- and first-order coefficients, c_0 and c_1 respectively, for the perturbative condensate, Eq. (14), for representative values of the bare quark mass parameter am_0 in lattice units. The uncertainties are from a numerical evaluation of the lattice perturbation theory loop integrals.

am_0	c_0	c_1
0.088	0.37962(2)	0.02561(12)
0.079	0.38029(1)	0.02709(13)
0.0728	0.38075(1)	0.02793(16)
0.067	0.38113(1)	0.02902(18)
0.062	0.38146(1)	0.02963(14)
0.0564	0.38178(1)	0.03049(22)
0.0505	0.38212(1)	0.03139(16)
0.0448	0.38240(1)	0.03203(18)
0.0386	0.38271(1)	0.03267(20)
0.032	0.38296(1)	0.03349(24)
0.028	0.38313(1)	0.03421(21)
0.024	0.38325(1)	0.03424(21)
0.020	0.38336(1)	0.03548(26)
0.016	0.38347(2)	0.03545(34)
0.01044	0.38356(1)	0.03614(49)
0.00507	0.38364(2)	0.03631(31)

used. A representative sample of our results is given in Table III, and is illustrated in Fig. 3.

An excellent fit to the perturbative coefficients in this range of small quark masses, $am_0 \lesssim 0.1$, can be obtained using the following parametrizations:

$$c_0(am_0) = c_{00} + (am_0)^2[c_{01}\log(am_0) + c_{02}], \quad (14)$$

and

$$c_1(am_0) = c_{10} + (am_0)^2[c_{11}\log^2(am_0) + c_{12}\log(am_0) + c_{13}]. \quad (15)$$

Higher order terms in am_0 appear as discretization errors in the comparison to $\overline{\text{MS}}$ to be done below and so can be ignored—they are negligible for the masses we are using in any case. The leading logarithm of am_0 at each order originates entirely from the infrared region of the loop momenta, and the respective coefficients c_{01} and c_{11} can easily be computed analytically. The values of these coefficients must and do agree with the values in the $\overline{\text{MS}}$ scheme [19]. At one loop we also have a constraint on the subleading (single) logarithm of am_0 since, as discussed in Appendix C, all $\log m$ terms must vanish in the difference between the vacuum expectation values of $m\bar{\psi}\psi$ in perturbation theory in the continuum and on the lattice. Allowing for the renormalization between the $\overline{\text{MS}}$ mass and the HISQ bare mass:

$$\bar{m}(\mu) = m_0\left(1 + \alpha_s\left[-\frac{2}{\pi}\log a\mu + 0.1143(3)\right] + \cdots\right), \quad (16)$$

we find that c_{12} should have the value 0.2307(2). With the logarithmic terms fixed to their known values we can
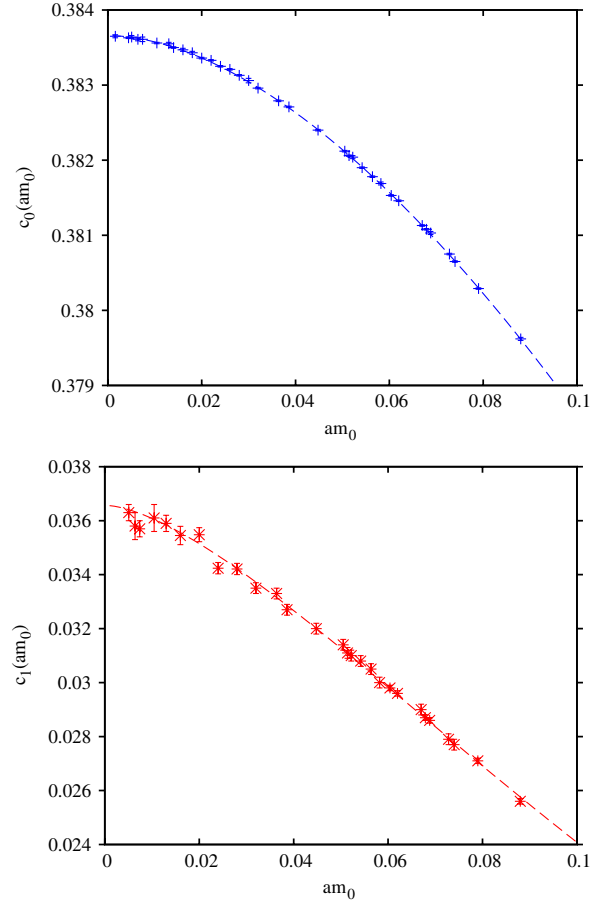

FIG. 3 (color online). Zeroth- and first-order coefficients, c_0 and c_1 respectively, for the perturbative condensate, Eq. (14), versus the bare quark mass parameter am_0 in lattice units. The uncertainties in c_0 resulting from numerical evaluations of the lattice loop integral are not visible in that plot. The fits given in the text are plotted as dashed lines.

obtain the other coefficients in Eqs. (14) and (15) from a fit to the values for $c_0(am_0)$ and $c_1(am_0)$ as a function of am_0. We find

$$c_{00} = 0.38366(1), \quad c_{01} = 3/(2\pi^2), \quad c_{02} = -0.153(1), \quad (17)$$

and

$$c_{10} = 0.03657(7), \qquad c_{11} = -6/\pi^3,$$
$$c_{12} = 0.2307(2), \qquad c_{13} = 0.308(15). \quad (18)$$

These fits are illustrated in Fig. 3 and reproduce our results for the coefficients to within their numerical integration errors, which are smaller than about 0.01% for c_0, and 1% for c_1.

The perturbative determination of the vacuum expectation value of $\bar{\psi}\psi$ has also been done in the $\overline{\text{MS}}$ scheme, in Ref. [19]. The power divergence is missing in this case but, as discussed above, there are terms proportional to $m^3\log m$. The authors of Ref. [19] find

$$-\langle\bar{\psi}\psi\rangle^{(\mu)}_{\mathrm{PT},\overline{\mathrm{MS}}} = \bar{m}^3(\mu)\times[d_{01}l_m + d_{02}$$
$$+ \alpha_s(d_{11}l_m^2 + d_{12}l_m + d_{13}) + \cdots], \quad (19)$$

where $l_m = \log(\bar{m}(\mu)/\mu)$ and

$$d_{01} = c_{01} = \frac{3}{2\pi^2}, \quad d_{02} = -\frac{3}{4\pi^2},$$
$$d_{11} = c_{11} = -\frac{6}{\pi^3}, \quad d_{12} = \frac{5}{\pi^3}, \quad d_{13} = -\frac{5}{2\pi^3}. \quad (20)$$

As discussed in Appendix B we must subtract the difference between the lattice QCD and $\overline{\mathrm{MS}}$ perturbative calculations from our lattice QCD results to obtain the nonperturbative condensate in the $\overline{\mathrm{MS}}$ scheme at the scale μ. We work with the combination $m\bar{\psi}\psi$ which would be renormalization group-invariant in the absence of this perturbative contribution and it is convenient to derive the subtraction needed in lattice units and as a function of the bare lattice quark mass. Using Eq. (16) we obtain

$$\Delta_{\mathrm{PT}} = -a^4(\langle m_0\bar{\psi}\psi\rangle_{\mathrm{PT,HISQ}} - \langle\bar{m}(\mu)\bar{\psi}\psi\rangle_{\mathrm{PT},\overline{\mathrm{MS}}})$$
$$= c_{00}(am_0)^2 + \alpha_s c_{10}(am_0)^2 + (am_0)^4[c_{01}l_\mu - 0.077(1)]$$
$$+ \alpha_s(am_0)^4[c_{11}l_\mu^2 + 0.1340(2)l_\mu + 0.406(15)] + \cdots,$$
$$(21)$$

where $l_\mu = \log(\mu a)$. This difference of perturbative expansions is now free of all logarithms of m and therefore well defined and infrared safe.

B. Determining the nonperturbative strange and light quark condensates

1. A first look at the results

The physical condensate in the $\overline{\mathrm{MS}}$ scheme at the scale μ is then defined by

$$\langle m\bar{\psi}\psi\rangle_{\mathrm{NP},\overline{\mathrm{MS}}}(\mu) = a^{-4}(a^4\langle m\bar{\psi}\psi\rangle_0 - \Delta_{\mathrm{PT}}), \quad (22)$$

where $\langle m\bar{\psi}\psi\rangle_0$ is the numerical result from lattice QCD and Δ_{PT} is given through $\mathcal{O}(\alpha_s)$ as a function of the quark mass in Eq. (21). Δ_{PT} will also contain unknown higher order pieces in α_s that we can try to determine from a fit to the lattice QCD results. First we look at the effect of the calculated tree-level and one-loop contributions.

Δ_{PT} is a strong function of the quark mass in lattice units, dominated by the $(ma)^2$ terms that give rise to the quadrative divergence with inverse lattice spacing. This means that the relative size of the subtraction compared to the raw results varies strongly with quark mass and with lattice spacing, and this is reflected in the raw results before the subtraction is made. In Fig. 4 the open squares show the unsubtracted results [i.e., setting Δ_{PT} to zero in Eq. (22)] as a function of the square of the inverse lattice spacing for quarks at the four different masses that we have results for in Table II: strange quarks and light quarks of masses $m_s/5$

(sets 1, 4 and 7), $m_s/10$ (sets 2 and 5) and the physical value, $m_s/27$ (sets 3, 6 and 8).

Instead of plotting the condensate results directly, the y axis in Fig. 4 is

$$R_l = -\frac{4m_l\langle\bar{\psi}\psi_l\rangle}{(f_\pi^2 M_\pi^2)} \quad (23)$$

for light quarks and

$$R_s = -\frac{4m_s\langle\bar{\psi}\psi_s\rangle}{(f_{\eta_s}^2 M_{\eta_s}^2)} \quad (24)$$

for strange quarks. The values of the raw unsubtracted R_q are determined directly from Table II using the am, aM, af and $\langle\bar{\psi}\psi\rangle_0$ values given there.

The ratio R_q is a good quantity to plot (and later to use in our fits) for a number of reasons:

(i) $m\langle\bar{\psi}\psi\rangle$ is a physical renormalization-group invariant quantity as $m \rightarrow 0$, up to discretization errors, as is clear from the GMOR relation. The division by the square of the meson decay constant times its mass makes a dimensionless ratio which is convenient but it is also one that (from the GMOR relation) we expect to be close to 1.

(ii) Using the ratio R_q also reduces the effect of any slight mistuning of quark masses since the quark mass multiplied in the numerator cancels against the square of the meson mass in the denominator. The tuning of m_s uses the η_s mass, and the determination of the lattice spacing uses f_{η_s}, as described in Ref. [23]. This means that, by definition, f_{η_s} does not contain discretization errors that would mask the identification of the pieces that diverge as $a \rightarrow 0$.

(iii) Finally the ratio has reduced finite-volume effects over that in either the numerator or denominator. This is expected from the fact that chiral loop effects, which are sensitive to the volume, cancel in R_q [28,29]. This is illustrated in Fig. 5 where we show results [30] for pion mass, decay constant and (unsubtracted) light quark condensate as well as the ratio R_l of Eq. (23) for ensembles with $am_{l,\mathrm{sea}} = 0.00507$ and $am_{s,\mathrm{sea}} = 0.0507$ and three different spatial volumes. The spatial volumes correspond to a spatial length in lattice units of 24, 32 and 40. The set with $L/a = 32$ is our set 4 (see Table I). For each quantity we plot the ratio of the value at $L/a = 32$ to that at $L/a = 40$. It is clear from the plot that the finite volume dependence in each of m_π, f_π and $\langle\bar{\psi}\psi\rangle_l$ is canceled to a very high level of accuracy [0.1(1)% for set 4] in R_l.

Figure 4 shows clearly the presence of a quadratic divergence with a^{-2} in the raw results. This is very "clean" in our calculations because the form of the divergence is very constrained. Only a term of the form m_q/a^2 is allowed in $\langle\bar{\psi}\psi\rangle$ for staggered quarks, i.e., no term of the
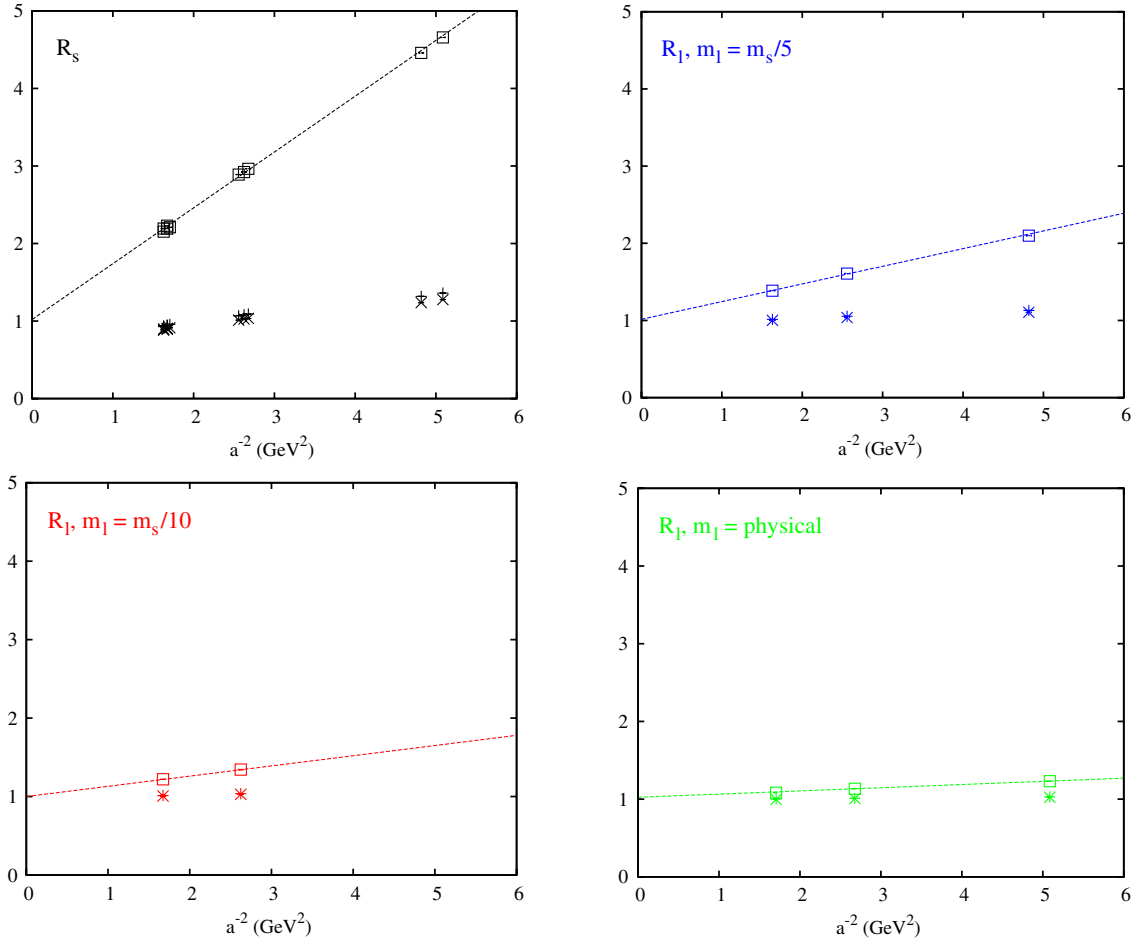
FIG. 4 (color online). R_q, defined as the ratio of quark mass times the condensate in the $\overline{\text{MS}}$ scheme at 2 GeV to the square of the meson mass times the decay constant, as a function of the square of the inverse lattice spacing. Left to right and top to bottom show strange quarks and light quarks with masses $m_s/5$, $m_s/10$ and the physical value. Squares use the unsubtracted condensate; pluses, the condensate after subtraction of the tree-level perturbative correction; and crosses, the condensate after perturbative correction through one loop. The value for α_s used to multiply the one-loop coefficient was $\alpha_V^{n_f=4}(2/a)$. Dashed lines illustrate very simple linear fits to the unsubtracted results as described in the text.

form m_q^2/a can appear. In the ratio R_q this term takes the form $C m_q^2/a^2$ where C depends on the meson mass and decay constant. The HISQ formalism has very small discretization errors, as is clear from the decay constant and meson mass results in Ref. [23], and so there is little additional a dependence to confuse the analysis of the divergent pieces.

Because the power divergence is so dominant it is tempting to try to fit the unsubtracted results for R_s to a very simple form: $A + B/a^2$. This is in fact possible (it is important to include the error in the inverse lattice spacing when doing this since this is larger than the error in R_q) and we obtain $1.02(3) + 0.725(3)/a^2$ which is the dashed line in the left-hand plot of Fig. 4. We also obtain $1.015(11) + 0.229(5)/a^2$ for R_l with $m_l = m_s/5$ and $1.00(1) + 0.130(6)/a^2$ for R_l with $m_l = m_s/10$, shown in the next two plots in Fig. 4. These fits are too naive to be useful, as we shall see below, because they ignore many important terms. Consequently

the value and error of the intercept, A, is unreliable for extracting a nonperturbative result for R_q, especially in the s quark case. However, the fits do illustrate that the ratio of slopes is that expected for a term that behaves as m_q^2/a^2 (although the simple fit does not allow for the running of the lattice bare quark mass with scale). The ratio of slopes between that for s and for l with $m_l = m_s/5$ is 3.2 which corresponds approximately to 5 (for the ratio of one power of the quark masses when the other power is canceled by the square of the meson mass) divided by the ratio of the square of the decay constants from Table II.

Figure 4 compares results for R_q in which the tree-level piece of Δ_{PT} has been subtracted from the raw values of $m\langle\bar{\psi}\psi\rangle$ following Eq. (22). We take μ to be 2 GeV. These results are indicated by pluses. Now the slope in a^{-2} is much smaller since most of the divergence has been removed. This makes the results more sensitive to the form of the remaining pieces of the divergence and the
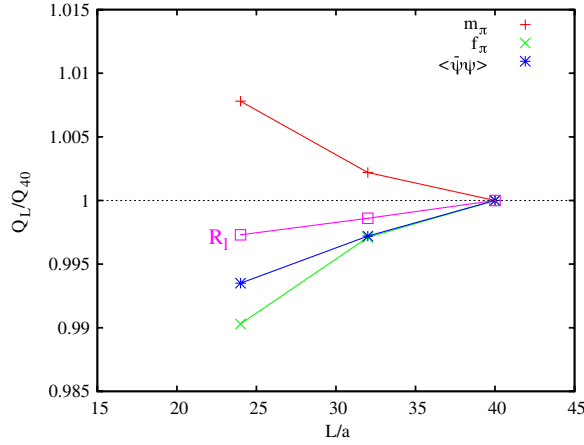
FIG. 5 (color online). Finite volume effects in different quantities are illustrated by plotting the ratio of the quantity on lattices of spatial length, L/a, of 24 and 32 to that on lattices of spatial length 40. The lattices have the sea quark mass parameters of coarse set 5. The quantities shown are the pion mass (red pluses), pion decay constant (green crosses) and unsubtracted light quark condensate (blue bursts). Pink squares give the result for the quantity R_l defined in Eq. (23) [30]. Statistical errors (not shown) are approximately 0.1%.

simple linear fits that were made to the unsubtracted data are no longer possible.

The $\mathcal{O}(\alpha_s)$ perturbative contribution is very small for HISQ quarks and makes very little difference to the perturbative subtraction. The crosses show the results taking Δ_{PT} to be the full calculated perturbative subtraction through $\mathcal{O}(\alpha_s)$ given in Eq. (21). We have used $\alpha_V^{n_f=4}(2/a)$ [31] for the α_s value multiplying the one-loop coefficient, but the coefficient itself is so small that variations in scale for α_s make no difference. The crosses are barely distinguishable from the pluses giving the tree-level subtracted numbers.

It is clear from Fig. 4 that there is still some divergence in a^{-2} left in R_q after subtraction of the perturbative contribution through one loop. This is not surprising since we know that Δ_{PT} will have higher order terms in α_s. The challenge now is to fit the one-loop subtracted R_q allowing for these higher order terms and thereby obtain the physical, nonperturbative results for the strange and light quark condensates. We will fit both R_s and R_l simultaneously and use the known mass dependence of the unknown higher order terms to constrain them. At the same time we will allow for higher order nondivergent mass dependent terms from perturbation theory as well as physical, nonperturbative dependence on the quark mass. Possible dependence on positive powers of a, i.e., discretization errors, must also be included.

2. Determining a physical result from fitting

We now describe the full fit to the results that we use to determine the final physical values for $\langle \bar{s}s \rangle$ ($\equiv \langle \bar{\psi}\psi_s \rangle$) and $\langle \bar{l}l \rangle$ ($\equiv \langle \bar{\psi}\psi_l \rangle$) at the physical strange and light quark

masses [where $m_l = (m_u + m_d)/2$]. We take the following form for the ratio R_q:

$$R_{q,0}(a, am_q) = R_{\mathrm{NP,phys}}^{(q)} + \delta R_{\mathrm{PT}} + \delta R_{a^2} + \delta R_\chi + \delta R_{\mathrm{vol}}.$$
(25)

$R_{q,0}$ are the raw results obtained from Table II; $R_{\mathrm{NP,phys}}$ is the final physical result in the $\overline{\mathrm{MS}}$ scheme at 2 GeV. The δR terms represent fitted or known dependence on a and am_q. We use Bayesian techniques [32] to perform the fits so that we can add many higher order terms as part of each δR with constrained coefficients. This makes sure that the final error on $R_{\mathrm{NP,phys}}$ is not underestimated by ignoring the existence of higher order corrections.

δR_{PT} contains the known tree-level and one-loop perturbative results given in Sec. III A. In addition we include unknown higher order terms. For the a^{-2} divergence these take the form

$$\delta R_{\mathrm{PT,div}} = a_n \frac{4\alpha_s^n(am_q)^2}{(af_\pi)^2(aM_\pi)^2}$$
(26)

with the analogous term for the strange quark case, with the same a_n. a_n is a coefficient whose prior we take to be 0.0 ± 4.0 and we allow for $n = 2, 3$ and 4. Note that a prior width of 4.0 is conservative given the size of the corresponding coefficient at tree level and one loop. For the nondivergent pieces we take

$$\delta R_{\mathrm{PT,non\text{-}div}} = c_n \frac{4\alpha_s^n(am_q)^4}{(af_\pi)^2(aM_\pi)^2}$$
(27)

again with the analogous term for the strange quark case, with the same coefficient c_n. We take $n = 2, 3$ and 4. c_n in principle contains a sum of powers of $\log(a\mu)$ up to $\log^{n+1}(a\mu)$. However, since $\log(a\mu)$ is small for $\mu = 2$ GeV and our range of lattice spacings, these pieces are negligible and do not affect the fit and we simply take a prior on c_n of 0.0(4.0). Again this is conservative given the results at tree level and one loop. For α_s we use $\alpha_V^{n_f=4}(2/a)$ [31] and discuss below the dependence of the results on changing $2/a$ to a different scale. $\alpha_V^{n_f=4}(2/a)$ takes values from 0.35 on the very coarse lattices to 0.26 on the fine ensembles.

δR_{a^2} allows for discretization errors. We take the form

$$\delta R_{a^2} = \sum_{i=1}^{2} d_i \left(\frac{\Lambda a}{\pi}\right)^{2i}.$$
(28)

Only even powers of a appear in discretization errors for staggered quarks and we take their scale to be set by $\Lambda \approx 1$ GeV. Since all tree-level errors at $\mathcal{O}(a^2)$ are removed in the HISQ formalism we take the prior for d_1 to be $\mathcal{O}(\alpha_s)$ i.e., 0.0(0.3). Higher order d_i are given the prior 0.0(1.0). We include a^2 and a^4 terms, but have checked that higher order terms have very little effect. In addition we include a mass dependent discretization error in the form $e(am)^2$,

giving e a prior of 0.0(1.0). This allows for a number of effects, one of which could be mixing with a gluon condensate. This has negligible impact.

δR_χ includes the valence and sea quark mass dependence that allows us to extrapolate to physical light quark masses and interpolate between the strange quark masses that we have to the physical strange quark mass. The chiral corrections to the GMOR relation were analyzed in Ref. [28] (see also Ref. [29]). The leading corrections are particularly simple because the chiral logarithms cancel to leave a correction proportional to M_π^2. We allow for both M_π^2 and M_π^4 terms in our light quark mass fits by defining a chiral expansion parameter

$$x_l = \frac{M_\pi^2}{2(\Lambda_\chi)^2}, \qquad (29)$$

with $\Lambda_\chi = 1.0$ GeV, and taking

$$\delta R_{\chi,\text{val}} = \sum_{i=1}^{2} g_i^{(l)} x_l^i. \qquad (30)$$

We fit the $m_q = m_s/5$, $m_s/10$ and $m_{l,\text{phys}}$ results with this form taking the prior on the g_i coefficients to be 0.0(2.0). This allows for a linear term of approximately the size expected in Ref. [29]. Higher order terms than x_l^2 have no effect.

The chiral expansion of Eq. (30) combines with the $R_{\text{NP,phys}}$ parameter in Eq. (25) to define the physical nonperturbative light condensate with its mass dependence. Since the GMOR relation is exact as $m_q \to 0$ we enforce this by taking the prior on $R_{\text{NP,phys}}^{(l)}$ to be 1.0000(5). Differences from 1 because of residual lattice finite volume effects up to 0.5% are allowed for as described in the paragraph above.

The data for R_s are fit simultaneously with that for the light quarks, because they share parameters for the perturbative subtraction. However, we largely decouple the physical parameters because the strange quark is relatively far from the chiral limit and we would need a lot of parameters for a chiral expansion to connect light and strange quarks. Instead we allow a separate parameter for $R_{\text{NP,phys}}^{(s)}$ with the broad prior of 1.0(5). We take the same form for the valence mass dependence as in Eq. (30) where now

$$x_s = \frac{(M_{\eta_s}^2 - (0.6893(12))^2)}{2(\Lambda_\chi)^2}, \qquad (31)$$

but this now simply allows for slight mistuning of the strange quark on some ensembles, and the fact that we have two values for the strange quark mass on sets 1 and 2. 0.6893 is the physical value for the η_s mass determined in Ref. [23]. The priors on $g_i^{(s)}$ are the same as those on $g_i^{(l)}$. Finite volume effects are expected to be completely

negligible for R_s because they are negligible for the components of R_s.

The strange quark results in Fig. 4 show some very small sensitivity to the sea light quark masses if we compare results on sets 1 and 2 and sets 3 and 4. We therefore allow an additional linear dependence on the light quark mass in the sea in δR_χ of the form

$$\delta R_{\chi,\text{sea}} = \sum_{i=1}^{2} k_i \left(\frac{\delta m_{\text{sea}}}{10 m_{s,\text{phys}}} \right)^i, \qquad (32)$$

where

$$\delta m_{\text{sea}} = (2m_{l,\text{sea}} + m_{s,\text{sea}}) - (2m_{l,\text{phys}} + m_{s,\text{phys}}). \qquad (33)$$

We take $m_{l,\text{phys}} = m_s/27.4$ [33] and $m_{s,\text{phys}}$ values determined from M_{η_s} as in Ref. [23]. The prior for coefficient k_i is taken as 0.0(1.0) which is conservative given the small effects observed in the results. We take $\delta R_{\chi,\text{sea}}$ to be common to both R_s and R_q for the light quarks. We note here also that the absence of chiral loop effects at this order means that staggered quark taste-changing effects are also absent. They can be handled, if necessary, with a sea quark mass dependent a^2 term [23]. Including such a term here makes no difference to the physical result.

δR_{vol} allows for remaining finite volume effects. These are small, as demonstrated in Fig. 5. They do produce a small systematic effect, however, because the lattice size in units of the pion mass, $M_\pi L$, is somewhat smaller on the lattices with smallest $m_{u/d}$. We take

$$\delta R_{\text{vol}} = v e^{-ML}, \qquad (34)$$

where M is the pseudoscalar meson mass made of that quark (M_π for R_l and M_{η_s} for R_s) and L is the linear extent of the lattice from Table I. Coefficient v is taken to have prior 0.0(0.2), consistent with Fig. 5.

Fitting results for R_s and R_q, $m_q = m_s/5$, $m_s/10$ and $m_{l,\text{phys}}$ simultaneously to the form in Eq. (25) readily produces good fits with $\chi^2/\text{d.o.f.} \approx 0.8$ for 18 degrees of freedom. The final fitted result for $R_{u/d}$ and R_s (evaluated from $R_{\text{NP,phys}}^{(q)}$ and δR_χ taken at the appropriate physical masses) is robust to the addition of higher order terms in the various corrections.

We take our final results from using $2/a$ for the scale of α_s. The results do not change significantly as the scale is varied (although the fitted coefficients a_n do change). Our fits return a substantial value for the coefficient of the power divergent term at $\mathcal{O}(\alpha_s^2)$, a_2, of around 2.0, for $d/a = 2/a$. This is substantially larger than that seen at one loop but not a particularly large value for a perturbative coefficient in general. It would simply imply that the small coefficient at one loop for the HISQ action is not repeated at higher orders. We also find that the chiral correction to the GMOR for light quarks is substantial and negative [$g_1^{(l)} = -1.7(6)$]. This will be discussed further below.
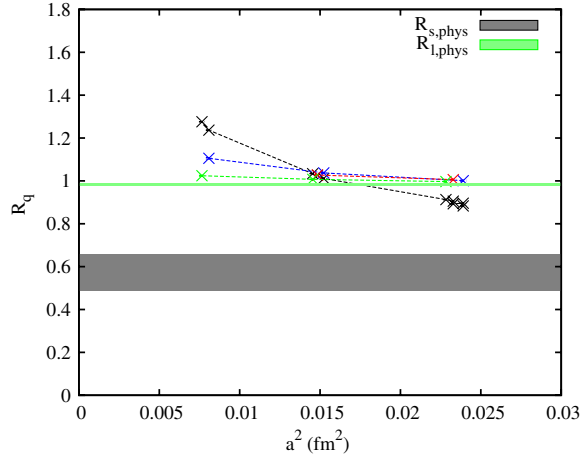
FIG. 6 (color online). Results from fitting the ratio R for three different quark masses as described in the text. The crosses show the lattice QCD results after subtracting the perturbative values through $\mathcal{O}(\alpha_s)$. Black is for s quarks, blue for quarks with mass $m_s/5$, red for quarks with mass $m_s/10$ and green for quarks at the physical light quark mass. The dashed lines simply join the points of matching color for clarity. The filled bands show the physical curves for strange (black) and light (green) quarks, once the full subtraction of the fitted perturbative contribution is made and masses are set to their physical values. The bands include the full error from the fit.

The fit results are shown in Fig. 6. The data points (crosses) correspond to the lattice QCD results after subtraction of the perturbative contribution through $\mathcal{O}(\alpha_s)$ (as in Fig. 4). The filled bands show the fitted curves when the full fitted perturbative contribution ($\delta R_{\rm PT}$) is subtracted and masses and decay constants are set to the physical values corresponding to the s quark and the light quark (for this we use $M_\pi = M_{\pi^0}$). These bands include the full error from the fit.

Our final physical results for R_q are the key results from this paper.

$$R_{l,\rm phys} = -\frac{4m_l \langle \bar{\psi}\psi_l \rangle_{\overline{\rm MS}}(2\ {\rm GeV})}{(f_\pi^2 M_\pi^2)},$$

$$R_{s,\rm phys} = -\frac{4m_s \langle \bar{\psi}\psi_s \rangle_{\overline{\rm MS}}(2\ {\rm GeV})}{(f_{\eta_s}^2 M_{\eta_s}^2)}. \qquad (35)$$

We find

$$R_{s,\rm phys} = 0.574(86)$$
$$R_{l,\rm phys} = 0.985(5) \qquad (36)$$
$$\frac{R_{s,\rm phys}}{R_{l,\rm phys}} = 0.583(84).$$

The complete error budgets for $R_{s,\rm phys}$, $R_{l,\rm phys}$ and their ratio are given in Table IV. The substantial 15% error that we have in $R_{s,\rm phys}$ reflects the difficulty of extracting a physical result from a power divergent quantity. For R_l

TABLE IV. Error budget for the quantities $R_{s,\rm phys}$, $R_{l,\rm phys}$ and their ratio defined in the text. Errors are given as percentages of the final physical result.

	$R_{s,\rm phys}$	$R_{l,\rm phys}$	$\frac{R_{s,\rm phys}}{R_{l,\rm phys}}$
Statistics	6.1	0.2	5.1
Lattice spacing	10.0	0.3	9.7
Finite volume	1.5	0.03	1.5
α_s value	1.7	0.06	1.7
Fitting power divergence	7.5	0.3	7.2
Other perturbative subtraction	1.3	0.07	1.3
χal extrapolation/interpolation (m_s)	3.0	0.1	2.9
χal extrapolation/interpolation (m_l)	4.5	0.2	4.3
$a \to 0$ extrapolation	1.9	0.05	1.9
Sea mass effects	0.5	0.01	0.5
Total	15	0.5	14.5

the error is 17 times better largely because the slope of the divergent piece is 15 times smaller. Errors in $R_{s,\rm phys}$ are dominated by errors from the lattice spacing and from fitting the remaining power divergent subtraction terms. There are also substantial errors from statistics and from tuning to the light and strange physical mass points. This is done by tuning the appropriate meson masses through the term $\delta R_{\chi,\rm val}$ in Eq. (30). This term depends on the lattice spacing through the definition of x_l [Eq. (29)] and x_s [Eq. (31)], because the meson masses appear in GeV units in these terms. The uncertainties in these terms then become correlated with the fit to the power divergence, increasing the uncertainty. For R_l the power divergence is much less of an issue, but these same terms dominate the final error there as well.

The results for R_l and R_s can be converted to values of the condensate using the lattice result for $f_{\eta_s} = 0.1819(5)$ GeV and $M_{\eta_s} = 0.6893(12)$ GeV [23], and experimental values for f_π [0.1304(2) GeV] and M_π (0.13498 GeV). We obtain

$$m_s \langle \bar{\psi}\psi \rangle_s^{\overline{\rm MS}}(2\ {\rm GeV}) = -2.26(34) \times 10^{-3}\ {\rm GeV}^4,$$
$$m_l \langle \bar{\psi}\psi \rangle_l^{\overline{\rm MS}}(2\ {\rm GeV}) = -7.63(4) \times 10^{-5}\ {\rm GeV}^4. \qquad (37)$$

The ratio of the two values above is slightly more accurate than a naive combination, giving 29.6(4.3).

Using the precise determinations for light quark masses now available from lattice QCD we can finally obtain condensate values. We take $m_s^{\overline{\rm MS}}(2\ {\rm GeV}) = 92.2(1.3)$ MeV [31,34] and $m_s/m_l = 27.41(23)$ [33,35]. These give

$$\langle \bar{s}s \rangle^{\overline{\rm MS}}(2\ {\rm GeV}) = -0.0245(37)(3)\ {\rm GeV}^3$$
$$= -(290(15)\ {\rm MeV})^3,$$
$$\langle \bar{l}l \rangle^{\overline{\rm MS}}(2\ {\rm GeV}) = -0.0227(1)(4)\ {\rm GeV}^3$$
$$= -(283(2)\ {\rm MeV})^3, \qquad (38)$$

where the second error for each condensate in GeV^3 comes from the error in the quark masses.

For the ratio of strange to light condensate we have

$$\frac{\langle \bar{s}s \rangle^{\overline{MS}}(2 \text{ GeV})}{\langle \bar{l}l \rangle^{\overline{MS}}(2 \text{ GeV})} = 1.08(16)(1), \tag{39}$$

where the first error comes from R_s/R_l and has the error budget given in Table IV and the second error comes from the strange to light quark mass ratio.

3. Approach of R to the chiral limit

The relationship of the light quark condensate to the chiral condensate is also important. R_q is defined to have the value 1 from the GMOR relation in the chiral limit but the results of Eq. (36) indicate that it approaches this limit from below as the light quark mass is reduced. Supporting evidence for this is found by studying the quantity R_δ derived from the combination of condensates used by the HOTQCD collaboration in their study of finite temperature QCD [36]. We define R_δ by

$$R_\delta = \frac{4m_l}{f_\pi^2 M_\pi^2} \frac{\langle \bar{\psi}\psi_l \rangle - \frac{m_l}{m_s}\langle \bar{\psi}\psi_s \rangle}{1 - \frac{m_l}{m_s}}. \tag{40}$$

The quadratic divergence with lattice spacing cancels between the two condensates because it is linear in the quark mass to all orders in perturbation theory. The non-divergent perturbative contributions proportional to the cube of the quark mass are completely negligible here, from the perturbative analysis in Sec. III A, and so we do not need to include them in making R_δ a physical quantity. R_δ can then simply be calculated from the raw data in Table II.

A plot of R_δ against m_l/m_s is shown in Fig. 7. In the $m_l \rightarrow 0$ limit on an infinite volume $R_\delta \rightarrow 1$ as R_l does. R_δ can be determined more precisely than R_l, however, because of the nonperturbative cancellation of the power divergence and it clearly approaches 1 from below. R_δ differs from R_l by a term which is proportional to m_l/m_s and to the difference between $\langle \bar{s}s \rangle$ and $\langle \bar{l}l \rangle$. Both the dependence of R_l on m_l and the difference between R_δ and R_l then contribute to the slope with m_l seen in Fig. 7. We cannot separate them and therefore unambiguously identify the slope of R_l with m_l. We can however use this for a consistency check.

We fit R_δ to the simple form:

$$R_\delta = 1.000(1) + c_1(1 + c_2 a^2 + c_3 a^4)\frac{m_l}{m_s} + c_4\left(\frac{m_l}{m_s}\right)^2$$
$$+ c_5 e^{-m_\pi L}. \tag{41}$$

This allows for linear and quadratic terms in m_l with discretization errors. We take priors on c_1, c_3 and c_4 to be 0.0(1.0) and the prior on c_2 to be 0.0(0.3), consistent with $\alpha_s a^2$ behaviors. The final term allows for finite
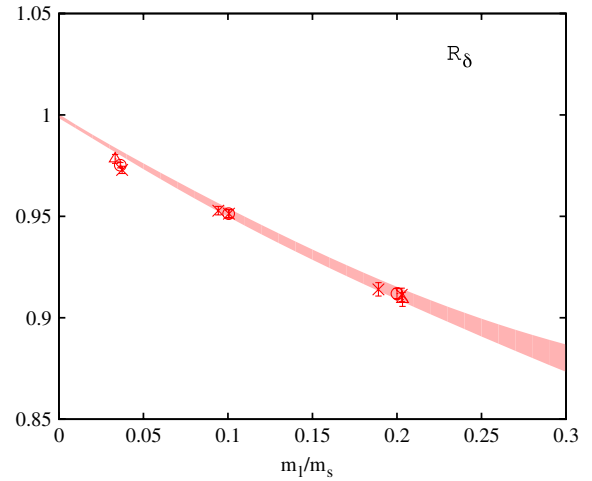

FIG. 7 (color online). R_δ as a function of m_l/m_s at three values of the lattice spacing. Points show the raw lattice results: the crosses are from very coarse lattices (sets 1 and 2 with two values of m_s on each and set 3), open circles from coarse lattices (sets 4, 5 and 6) and open triangles from fine sets 7 and 8. The shaded band gives the results of a simple fit incorporating discretization and finite volume effects as described in the text.

volume effects dependent on the combination $m_\pi L$. As for our fit to R_l, we take the prior on c_5 to be 0.0(0.2) for consistency with Fig. 5.

The fit gives $\chi^2/\text{d.o.f.}$ of 0.75 for 10 degrees of freedom and a physical slope, c_1, of $-0.51(4)$. This value is consistent with the difference between R_l and 1 in Eq. (36), and indeed with the difference between R_s and 1. This consistency between the results from R_δ and R_l indicates that the difference between $\langle \bar{s}s \rangle$ and $\langle \bar{l}l \rangle$ (which would upset this consistency) cannot be large. This is indeed what we also find in Eq. (39).

4. The chiral susceptibility

A further quantity that is of particular interest in studies of QCD at finite temperature is the chiral susceptibility for a quark of flavor f:

$$\chi_f = \frac{\partial}{\partial m_f}(-\langle \bar{\psi}\psi_f \rangle). \tag{42}$$

We give results here for the chiral susceptibility for zero temperature QCD to fill out the physical picture of the condensate. From differentiation of the path integral for the condensate it is clear that the chiral susceptibility is given by the flavor-singlet scalar correlator. It is convenient to split this into two contributions which we call χ_q and χ_g.[1] χ_q comes from two scalar operators connected by quark lines, which is the flavor-nonsinglet scalar meson correlator. χ_g comes from two scalar operators connected only by gluons, in which the disconnected contribution is canceled.

---

[1]In Ref. [36] these are called χ_{conn} and χ_{disc}.
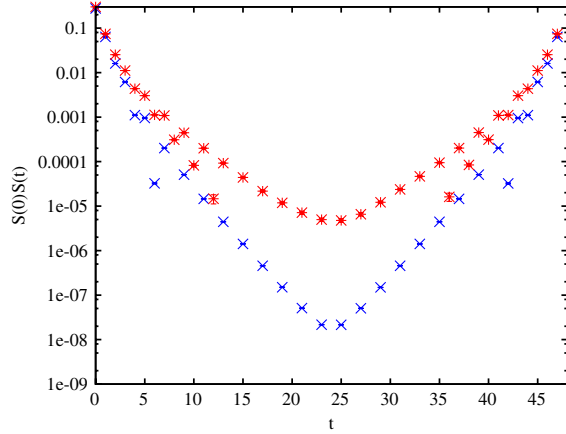
FIG. 8 (color online). Results for the quark-line connected scalar correlator on set 1: s quarks (blue crosses) and light quarks with $m_l = m_s/5$ (red bursts). The sum over time of this correlator is χ_q. Negative values of the correlator are not plotted on this log scale.

$$\chi = \chi_q + \chi_g, \qquad \chi_q = \frac{1}{N_t}\sum_n \text{Tr}[M_{0n}^{-1}M_{n0}^{-1}],$$

$$\chi_g = -\frac{1}{N_t^2 V}(\langle(\text{Tr}M^{-1})^2\rangle - \langle\text{Tr}M^{-1}\rangle^2). \tag{43}$$

The factors of the number of tastes, N_t, above are specific to naive/staggered quarks.

χ_q is readily calculated by generating quark propagators with the same random wall source of noise as that used for the π and η_s mesons, but patterned with phases that are -1 on all odd sites on an even-odd partitioning of the lattice. We then combine one of these propagators with the matching one used in the π/η_s meson, again multiplying the odd sink sites with a phase of -1. Summing over spatial sites at each time slice gives the flavor-nonsinglet scalar correlator. Examples are shown in Fig. 8. Summing this correlator over time slices gives χ_q. Results for χ_q for light and strange quarks on sets 1 and 4 are given in Table V.

χ_g can be estimated from our existing results for the light and strange condensates. Because we have 16 time sources for our propagators we can determine the correlation between $\text{Tr}M^{-1}$ operators that are n time slices apart where n is a multiple of 3 for set 1 and a multiple of 4 for set 4. This gives a correlation function, for example that

TABLE V. Contributions to the chiral susceptibility, defined in Eq. (44) for very coarse set 1 and coarse set 4 for light ($m_l = m_s/5$) and strange quark masses.

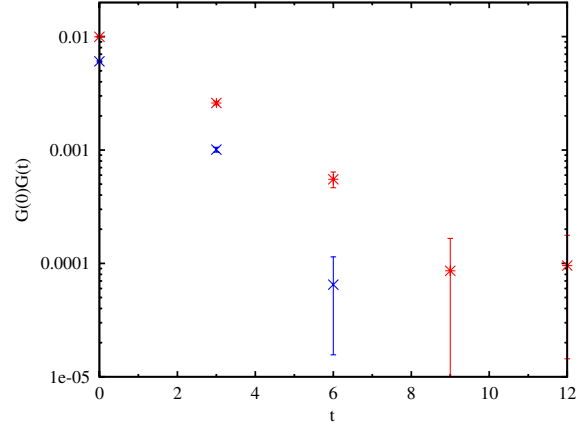| Set	ma	$a^2\chi_q$	$a^2\chi_g$
1	0.013	0.54296(36)	0.045(14)
	0.0688	0.45359(6)	0.021(7)
3	0.01044	0.50850(18)	0.032(10)
	0.0522	0.46231(3)	0.014(4)

FIG. 9 (color online). Results for the gluon-connected contribution to the scalar correlator on set 1 for s quarks (blue crosses) and light quarks with $m_l = m_s/5$ (red bursts). The sum over time of this correlator is χ_g.

shown in Fig. 9. χ_g is then the sum over time slices of this correlation function. We can estimate χ_g in several ways. Our central result comes from estimating an effective mass from the early time slices that dominate χ_g and where we have a strong signal. We can then reconstruct an estimated correlation function and sum over it. We can also simply sum over the correlator for the time slices that we have and multiply by 3 or 4 as appropriate. From this range of methods we estimate the error in χ_g as 30%. Values are given in Table V. χ_g is much smaller than χ_q.

The quantities that are almost renormlization-group invariant, that we can compare, are $m_f^2\chi_f$ and $m_f(-\langle\bar\psi\psi\rangle_f$). This is done in Fig. 10. Both of these quantities contain the same power divergence (proportional to $m_f^2 a^{-2}$) in the lattice spacing. In the susceptibility this divergence largely comes from χ_q. The nondivergent perturbative contributions to the two quantities will be different but, as we have seen, they are very small and we ignore them here.

We find that the difference between $m_f^2\chi_f$ and $-m_f\langle\bar\psi\psi\rangle_f$, also plotted in Fig. 10, does not depend on the lattice spacing within errors. We simply average over the results at the two values of the lattice spacing to obtain physical results for

$$m_f\left(1 - m_f\frac{\partial}{\partial m_f}\right)\langle-\bar\psi\psi_f\rangle. \tag{44}$$

The values are $2.18(7) \times 10^{-3}$ GeV^4 for s quarks and $3.93(9) \times 10^{-4}$ GeV^4 for light quarks with $m_l = m_s/5$. Comparison of these numbers with the physical results for $m_f\langle\bar\psi\psi\rangle_f$ given in Eq. (37) allows us to determine the value and sign of $m_f^2\chi_f$. For s quarks the comparison is straightforward and we find

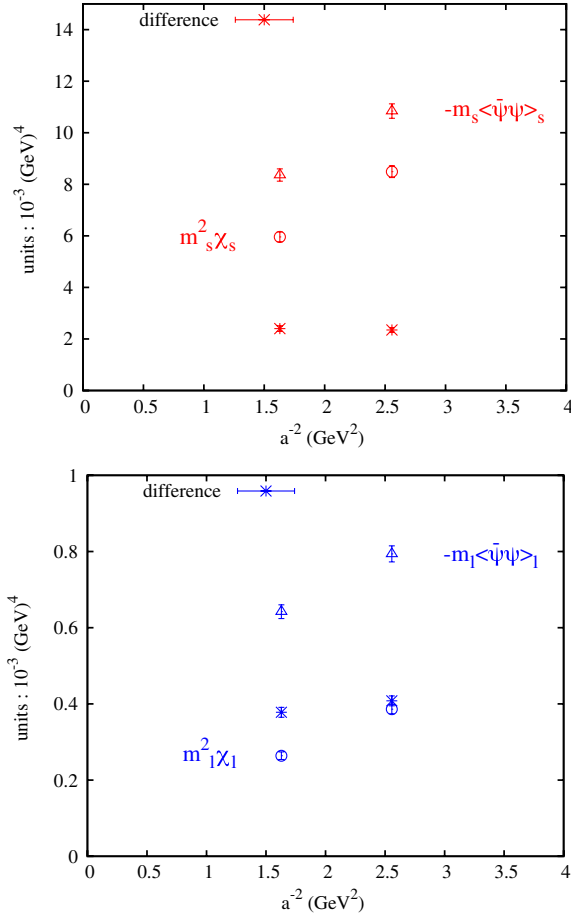$$m_s^2\chi_s = 0.08(35) \times 10^{-3} \text{ GeV}^4, \tag{45}$$

consistent with zero.

FIG. 10 (color online). Results for $m_f^2 \chi_f$ (open circles) compared to $m_f \langle \bar{\psi} \psi_f \rangle$ (open triangles) as a function of the square of the inverse lattice spacing, for s quarks (top) and light quarks with $m_l = m_s/5$ (lower plot). Results are for sets 1 and 4. Bursts show the difference of these two quantities.

To obtain a value for $m_l^2 \chi_l$ at $m_l = m_s/5$ we need a result for $m_l \langle \bar{\psi} \psi_l \rangle$ at this mass. Our fit in Sec. III B 2 gives a result for $R_{l=s/5}$ of 0.915(26). At this value of m_l we have $M_\pi = 315$ MeV and can estimate $f_\pi = 145$ MeV from our results in Table II. Then $m_{l=s/5} \langle \bar{\psi} \psi_{l=s/5} \rangle = 4.78(20) \times 10^{-4}$ GeV^4. In the error we have included an interpolation error for each mass and decay constant of 1%. Then, subtracting the result for the difference of Eq. (44) at $m_l = m_s/5$ given above, we have

$$m_{l=s/5}^2 \chi_{l=s/5} = 0.85(22) \times 10^{-4} \text{ GeV}^4, \qquad (46)$$

which is a small positive slope.

Our results are then consistent with a slope in $\langle \bar{\psi} \psi_f \rangle$ with m_f that is positive at $m_s/5$ but may decrease or even become negative by m_s. If the slope at $m_s/5$ remained constant for larger m_f it would give a total change in $\langle \bar{\psi} \psi_f \rangle$ of 3×10^{-3} between $m_s/5$ and m_s which is not inconsistent with the change of $1.8(3.8) \times 10^{-3}$ that we find in Eq. (38).

IV. DISCUSSION

We have determined a physical value for the strange quark condensate from lattice QCD for the first time. This required both nonperturbative lattice QCD results and a perturbative determination of the power divergent contribution through $\mathcal{O}(\alpha_s)$. The calculation relies on the good chiral properties of staggered quarks to control the form of the power divergence and the numerical speed and small discretization of the highly improved staggered quark formalism to allow very precise results to be obtained at several values of the lattice with light u/d sea quark masses. We proceed by tracking deviations from the GMOR relation, making extensive use of our previous work determining the physical properties of the η_s meson, to obtain the strange quark condensate. Our best result comes from gluon field configurations that include u, d, s and c quarks in the sea. The condensate is given in the $\overline{\text{MS}}$ scheme at a scale of 2 GeV. The evolution equation required to run $m \langle \bar{\psi} \psi \rangle$ to other scales, since it is not renormalization group-invariant, is given in Appendix B. We obtain a very consistent result for the strange quark condensate from independent calculations that include $2 + 1$ favors of sea quarks, as discussed in Appendix D.

Our value is $-(290(15) \text{ MeV})^3$ giving a ratio of strange to light condensates of 1.08(16). Earlier results come from sum rules of various kinds. These show significant variation and often have no estimate of the error associated with the value. Narison [37] gives a compilation with a final value for the ratio of strange to light condensates in the $\overline{\text{MS}}$ scheme at a scale of 2 GeV of 0.75(12). A value of 0.74(3) is quoted from baryon mass splittings in Ref. [11]. Finite energy sum rules in the kaon sector give a ratio 0.6(1) in Ref. [38]. More recently Maltman [12] uses sum rules for the ratio of decay constants f_{B_s}/f_B along with the 2007 lattice QCD average for this ratio of 1.21(4) [39,40] to obtain $\langle s\bar{s} \rangle / \langle l\bar{l} \rangle_{\overline{\text{MS}}}(2 \text{ GeV}) = 1.2(3)$. This updates an earlier result of 0.8(3) from Jamin [29] which used a quenched lattice QCD result for f_{B_s}/f_B of 1.16(4). The current lattice QCD world average for f_{B_s}/f_B is 1.20(2) [41].

Figure 11 compares our result for the strange to light condensate ratio with the results from sum rules discussed above. Our central value lies between the sum rules results, being in agreement with the larger value of Ref. [12] but only in marginal agreement with the lower values of Ref. [38]. A value below 0.6 is ruled out by our results at the 3σ level. Our value is more accurate than the result derived from f_{B_s}/f_B and has the advantage over all the sum rules results that it is a direct determination from QCD and has a full error budget (Table IV).

We obtain a very accurate value for the light quark condensate, giving $-(283(2) \text{ MeV})^3$. We can distinguish the ratio R_l at the physical light quark mass from that of 1 in the chiral limit using our results in Eq. (36). Defining δ_π from [29]
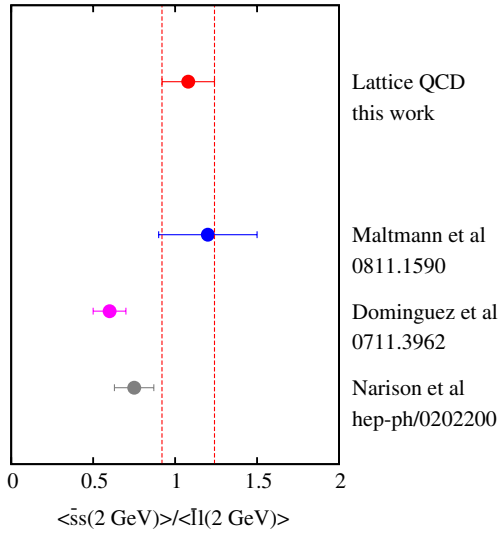
FIG. 11 (color online). A comparison of results for the ratio of strange to light condensates in the $\overline{\text{MS}}$ scheme at 2 GeV.

$$R_l = 1 - \delta_\pi \qquad (47)$$

we obtain a value $\delta_\pi = 0.015(5)$. This is somewhat lower than the value of 0.047(17) estimated in Ref. [29], although in agreement within 2σ. It is not in agreement with the somewhat larger number of 0.06(1) obtained in Ref. [42]. Our result implies a value for the combination $(2L_8^r - H_2^r)$ of low-energy constants from the chiral Lagrangian that is a factor of 3 lower than that used in Ref. [29]. The value is 3σ larger than zero, however.

Note that we do not expect the value of the light quark condensate to agree with that of the chiral (zero quark mass) condensate, Σ. The relationship between them is

$$\Sigma(2 \text{ GeV}) = \frac{-\langle \bar{l}l \rangle (2 \text{ GeV})}{R_{l,\text{phys}}} \frac{f^2}{f_\pi^2} \frac{(M^2/m)_{m=0}}{M_\pi^2/m_{l,\text{phys}}}. \qquad (48)$$

Here f is the decay constant in the zero quark mass limit and M^2/m is the ratio of the square of the pion mass to the light quark mass in the same limit. f_π/f can be determined from chiral extrapolation of lattice QCD results. For example, a recent accurate calculation [3] gives $f_\pi/f = 1.0627(28)$ including $2 + 1$ flavors of sea quarks. A preliminary analysis based on the results given here for $2 + 1 + 1$ sea flavors in Table II gives 1.056(1), in acceptable agreement. From the figures in Ref. [3] we estimate $(M^2/m)_{m=0}/(M_\pi^2/m_{l,\text{phys}})$ as 1.02. Combining these factors, along with R_l, into Eq. (48) makes clear that we expect a 3% difference between the magnitudes of $\Sigma^{1/3}$ and $(\langle \bar{l}l \rangle)^{1/3}$, dominated by the effect of f_π/f (so that Σ is smaller). This is entirely consistent, assuming no difference between $2 + 1$ and $2 + 1 + 1$ flavors of sea quarks, with the fact that we obtain $\langle \bar{l}l \rangle (2 \text{ GeV}) = -(283(2) \text{ MeV})^3$ and [3] obtain $\Sigma(2 \text{ GeV}) = (272(2) \text{ MeV})^3$ from a chiral analysis.

Other methods for determining Σ are not as accurate, but in reasonable agreement. We quote here two recent examples. JLQCD/TWQCD give a result of $(234(17) \text{ MeV})^3$ [43] from the eigenvalue spectrum of overlap quarks with u, d and s quarks in the sea. The ETM collaboration give $(299(38) \text{ MeV})^3$ [44] from fits to the Landau gauge quark propagator with u and d quarks in the sea. Additional lattice results for Σ are collected in Ref. [45].

Our analysis has implications for other calculations. For example:

(i) Finite temperature determinations of the chiral phase transition in QCD use an order parameter based on the light quark condensate. A nonperturbative subtraction is made with the aim of removing the power divergent pieces proportional to ma and with the assumption that the higher order $[(ma)^3]$ terms are negligible. For example the HOTQCD collaboration uses an order parameter [36] for visualizing the transition (fits to find the transition temperature also include other results) which is the ratio between nonzero and zero temperatures of

$$\langle \bar{\psi} \psi \rangle_l - \frac{m_l}{m_s} \langle \bar{\psi} \psi \rangle_s. \qquad (49)$$

This quantity becomes

$$\langle \bar{\psi} \psi \rangle_{l,\text{NP}} - \frac{m_l}{m_s} \langle \bar{\psi} \psi \rangle_{s,\text{NP}} \qquad (50)$$

if we assume only the presence of a power divergence linear in ma. Our analysis shows that this is a good assumption. For example, the difference between subtracting only terms linear in ma at tree level and including terms cubic in ma is 0.2% for the strange condensate on the coarsest HOTQCD lattices (i.e., those with the largest $m_s a$ values). Note however that the value in Eq. (50) differs from $\langle \bar{\psi} \psi \rangle_{l,\text{NP}}$ by an amount which could be worked out given the results in this paper.

An alternative approach might be to calculate $(1 - m\partial/\partial m)\langle \bar{\psi} \psi \rangle$ as discussed in Sec. III B 4. The quark-line connected piece of this can be calculated directly by combining the expression for χ_q in Eq. (44) and the expression for $\langle \bar{\psi} \psi \rangle$ in Eq. (10). The combination becomes [27]

$$\left(1 - \frac{\partial}{\partial m} \right)_{\text{conn}} \langle -\bar{\psi} \psi \rangle = 2m \sum_{n \text{ even}} \text{Tr}|M_{0n}^{-1}|^2. \qquad (51)$$

This can clearly be generalized to a sum over even source sites, implemented with a partial random wall. When combined with the quark-line disconnected piece χ_g this gives a physical quantity without power divergent pieces which is close to the value of the condensate itself.

(ii) The comparison of heavy-light current-current correlators to continuum QCD perturbation theory can be used to normalize heavy-light currents in lattice

QCD. The light quark condensate appears in this comparison and the results given here will enable us to improve the analysis in Ref. [8]. This is underway.

(iii) Some recent papers [46] have speculated that the quark condensate may only be nonzero inside hadrons. A much smaller value outside hadrons would significantly ameliorate the fine-tuning problem associated with the cosmological constant. This suggestion appears to be in conflict with direct calculations of quark condensates as vacuum expectation values described here.

V. CONCLUSIONS

We give the first direct determination of the strange quark condensate from lattice QCD, having demonstrated how to extract a well-defined physical value from lattice results that contain a power divergence as the lattice spacing goes to zero. Our results include a calculation through $\mathcal{O}(\alpha_s)$ in lattice QCD perturbation theory of the perturbative contribution to the condensate, part of which is the power divergence. The calculation relies on the good chiral properties of staggered quarks to control the form of the power divergence and the numerical speed and small discretization of the highly improved staggered quark formalism to obtain precise results at multiple lattice spacings and light quark masses. Our results include values at physical light quark masses.

We obtain a value for the strange quark condensate in the $\overline{\text{MS}}$ scheme at 2 GeV of $-(290(15)\,\text{MeV})^3$. We give a full error budget for this result in Table IV, the main sources of error being those associated with fitting and subtracting the remaining power divergence. The result includes u, d, s and c quarks in the sea but we get good agreement with this value from independent calculations that include u, d and s sea quarks only.

The value we obtain for the corresponding light quark condensate [where $m_l = (m_u + m_d)/2$] is $-(283(2)\,\text{MeV})^3$. Note that is significantly different from the value for the condensate in the chiral limit. The ratio of our light quark condensate to a recent lattice QCD value for the chiral condensate from Ref. [3] is 1.13(3), consistent with the behavior of meson masses and decay constants approaching the chiral limit.

We have shown that the ratio of four times the quark mass times the condensate divided by the square of the meson mass times the decay constant approaches the GMOR value (of 1) from below as $m_l \rightarrow 0$. At the physical light quark mass the value is 1.5% below 1, and at the strange mass it is 57% of 1.

Our result for the ratio of the strange condensate to the light quark condensate is 1.08(16). This sits in the middle of the spread of results from QCD sum rules but provides significant additional information because it is a direct determination with a full error budget. The result will have an impact on a number of other calculations both in the continuum and in lattice QCD. Some of the numerical techniques used here will be useful for determinations of, for example, the strangeness content of the pion or nucleon.

APPENDIX A: CONDENSATES FROM CORRELATORS

Equation (11) relates the zero-momentum pseudoscalar propagator to the scalar quark-condensate and is a well-known relationship [27]. The relationship is true (for the HISQ formalism) even on a single gluon configuration. Here, for completeness, we give a simple derivation, using the equivalent naive quark formalism.

The contribution to the propagator from a single gluon configuration is given by

$$G_{\text{ps}} \equiv \sum_x \text{Tr}\left[\gamma_5 \left(\frac{1}{D \cdot \gamma + m}\right)_{0x} \gamma_5 \left(\frac{1}{D \cdot \gamma + m}\right)_{x0} \right], \quad \text{(A1)}$$

where D is the gauge-covariant derivative, and the trace is over spin and color indices. The contribution to the scalar quark condensate is given by

$$S \equiv -\text{Tr}\left(\frac{1}{D \cdot \gamma + m}\right)_{00}. \quad \text{(A2)}$$

To extract the relationship, we multiply by the unit matrix under the trace in the condensate:

$$\begin{aligned}
S = &-\sum_{xy} \text{Tr}\left[(-D \cdot \gamma + m)_{0x} \left(\frac{1}{-D \cdot \gamma + m}\right)_{xy} \right.\\
&\left. \times \left(\frac{1}{D \cdot \gamma + m}\right)_{y0} \right]\\
= &-\sum_x \text{Tr}\left[(-D \cdot \gamma + m)_{0x} \left(\frac{1}{-(D \cdot \gamma)^2 + m^2}\right)_{x0} \right]. \quad \text{(A3)}
\end{aligned}$$

Only the m term in the numerator of the last expression survives the spinor trace since the other term results in traces of odd numbers of γ matrices (which vanish). Consequently

$$S = -m\text{Tr}\left(\frac{1}{-(D \cdot \gamma)^2 + m^2}\right)_{00}$$

$$= -m\sum_x \text{Tr}\left[\left(\frac{1}{-D \cdot \gamma + m}\right)_{0x}\left(\frac{1}{D \cdot \gamma + m}\right)_{x0}\right]$$

$$= -m\sum_x \text{Tr}\left[\gamma_5\left(\frac{1}{D \cdot \gamma + m}\right)_{0x}\gamma_5 \times \left(\frac{1}{D \cdot \gamma + m}\right)_{x0}\right]$$

$$= -mG_{\text{ps}}, \tag{A4}$$

which is Eq. (11). Since this relationship is true, configuration by configuration, it must be true of the ensemble averages as well.

Note that Eq. (A4) leads immediately to the GMOR relation [Eq. (1)]. To see this rewrite the pseudoscalar propagator in terms of its mesonic intermediate states. Only the pion contribution survives the $m \to 0$ limit, since the effective decay constants for excited states all vanish in that limit (by the Ward identity). The pion contribution has an amplitude $a = f_\pi^2 m_\pi^3/(4m)$ multiplied by an exponential decay in time, whose integral gives $1/m_\pi$.

The analysis of the propagator above only works for quark actions that have a γ_μ piece and a scalar piece (and nothing else), and where those two pieces commute with each other. The commuting is essential if you want

$$(-D \cdot \gamma + m)(D \cdot \gamma + m) = -(D \cdot \gamma)^2 + m^2 \tag{A5}$$

with only terms having an even number of γ_μ's on the right-hand side. So this proof does *not* work for Wilson's lattice discretization of the quark action or similar formulations. On the other hand, it is true of staggered-quark formalisms such as HISQ.

Equation (11) also follows directly from the (integrated) axial Ward identity:

$$\sum_x \langle(m_a + m_b)J_{ab}^5(x)(m_a + m_b)J_{ab}^{5\dagger}(0)\rangle$$

$$= -\langle(m_a + m_b)(\bar{\psi}_a\psi_a + \bar{\psi}_b\psi_b)\rangle \tag{A6}$$

with $J_{ab}^5 \equiv \bar{\psi}_a(x)\gamma_5\psi_b(x)$. This is exact on the lattice for lattice actions with sufficient chiral symmetry and again shows that Eq. (10) is an identity, true configuration by configuration and for any m_a and m_b. See Ref. [47] for a derivation using twisted mass quarks.

Here we have used the cases $m_a = m_b$ and both equal to either m_l or m_s but we can derive from Eq. (A6) a relationship [27] between correlators for the mixed Goldstone pseudoscalar made of light and strange quarks and the "diagonal" cases:

$$(am_l + am_s)\sum_t C_K(t) = (am_l)\sum_t C_\pi(t) + (am_s)\sum_t C_{\eta_s}(t). \tag{A7}$$

The left-hand side is then related to the sum of quark masses multiplied by the sum of quark condensates. This does not add new information so we do not make use of this relationship except as a test of our correlators.

APPENDIX B: CONDENSATES AND THE OPE

Condensates typically arise in the nonleading terms of operator-product expansions (OPE). To illustrate, consider moments of two pseudoscalar densities composed of a heavy quark (mass M) and a light quark (mass $m \ll M$) where the heavy quark fields are contracted with each other:

$$(m + M)^2 \int d\mathbf{x}dt\, t^n J_5(\mathbf{x}, t)J_5(0) \to \mathcal{O}^{(n)}, \tag{B1}$$

where

$$\mathcal{O}^{(n)} \equiv \int d\mathbf{x}dt\, t^n \bar{\psi}(\mathbf{x}, t)\gamma_5 \frac{(m + M)^2}{D \cdot \gamma + M}\gamma_5\psi(0), \tag{B2}$$

and ψ is the light-quark field. Lattice simulations of $\langle 0|\mathcal{O}^{(n)}|0\rangle$ can be used to determine the heavy quark's mass [48]. The $(m + M)^2$ factor makes $\mathcal{O}^{(n)}$ independent of the ultraviolet regulator provided $n \geq 4$; that is, lattice and continuum calculations should agree in the limit of zero lattice spacing.

Operator $\mathcal{O}^{(n)}$ is also a short-distance operator, dominated by length scales of order $1/M$, provided the heavy quark is sufficiently heavy and the light quarks have small momenta compared with M. Consequently the OPE implies that $\mathcal{O}^{(n)}$ can be expressed in terms of a set of local operators in an effective theory, with cutoff scale $\Lambda < M$, and coefficient functions that depend only upon physics between scales Λ and M:

$$\bar{M}^{n-4}\mathcal{O}^{(n)} = \mathbf{1}^{(\Lambda)}c(\Lambda/\bar{M}, \bar{\alpha}_s, \bar{m}/\bar{M})$$

$$+ \frac{(m\bar{\psi}\psi)^{(\Lambda)}}{\bar{m}\bar{M}^3}d(\Lambda/\bar{M}, \bar{\alpha}_s, \bar{m}/\bar{M}) + \cdots, \tag{B3}$$

where $\mathbf{1}^{(\Lambda)}$ is the unit operator and we have replaced $\bar{\psi}\psi$ by $m\bar{\psi}\psi$, to simplify the coefficient function. Somewhat arbitrarily, we have chosen to express the right-hand side in terms of masses and couplings at scale $\mu = M(\mu) \equiv \bar{M}$:

$$\bar{M} \equiv M(\bar{M}), \qquad \bar{m} \equiv m(\bar{M}), \qquad \bar{\alpha}_s \equiv \alpha_s(\bar{M}). \tag{B4}$$

The effective theory on the right-hand side of Eq. (B3) could be, for example, lattice QCD with a lattice spacing $a = \pi/\Lambda$, or QCD with an $\overline{\text{MS}}$ regulator and $\mu = \Lambda$.

The coefficient functions c and d are perturbative when M is large, and analytic in $\bar{\alpha}_s$ and $\bar{m}/\bar{M}$.[2] They can be computed using perturbative matching. For example, we can examine matrix elements of Eq. (B3) between low-energy, on-shell light-quark states $\langle q|$ and $|q'\rangle$. The unit operator drops out and Eq. (B3) can be rearranged to give

---

[2]We are ignoring nonperturbative short-distance physics (for example, small instantons) which can contribute to coefficient functions but is typically nonleading.

$$d(\Lambda/\bar{M}, \bar{\alpha}_s, \bar{m}/\bar{M}) = \left(\frac{\bar{m}\bar{M}^{n-1}\langle q|\mathcal{O}^{(n)}|q'\rangle}{\langle q|m\bar{\psi}\psi|q'\rangle^{(\Lambda)}}\right)_{\text{PQCD}}, \quad \text{(B5)}$$

where the right-hand side is computed order by order in perturbation theory. Since $\langle q|M\bar{\psi}\psi|q'\rangle$ is independent of Λ, d is actually regulator independent:

$$d = d(\bar{\alpha}_s, \bar{m}/\bar{M}). \quad \text{(B6)}$$

Knowing d, one would then compute c using perturbative expansions of the vacuum expectation values:

$$c(\Lambda/\bar{M}, \bar{\alpha}_s, \bar{m}/\bar{M})$$
$$= \left(\frac{\langle 0|\mathcal{O}^{(n)}|0\rangle}{\bar{M}^{4-n}} - \frac{\langle 0|m\bar{\psi}\psi|0\rangle^{(\Lambda)}}{\bar{m}\bar{M}^3}d(\bar{\alpha}_s, \bar{m}/\bar{M})\right)_{\text{PQCD}}. \quad \text{(B7)}$$

Equation (B7) underscores the importance of avoiding normal-ordered operators in operator-product expansions. Each term on the right-hand side has infrared sensitive contributions that go like $m^3 \log(m)$. These cancel between the two terms in Eq. (B7), order by order in perturbation theory; but this cancellation would have been ruined had we replaced $\bar{\psi}\psi$ by the normal-ordered product $:\bar{\psi}\psi:$ in Eq. (B3) (and c would no longer be perturbative).

It is also important to note that $\langle 0|m\bar{\psi}\psi|0\rangle^{(\Lambda)}$ is *not* cutoff independent, because of operator mixing with the unit operator $m^4\mathbf{1}$, which implies that

$$\frac{d\langle 0|m\bar{\psi}\psi|0\rangle^{(\Lambda)}}{d\log\Lambda} = \gamma_{\text{mix}}(\alpha_s(\Lambda), m(\Lambda)/\Lambda)m^4(\Lambda), \quad \text{(B8)}$$

where

$$\gamma_{\text{mix}}(\alpha_s) = \frac{3}{2\pi^2} + O(\alpha_s) \quad \text{(B9)}$$

depends upon the regulator scheme beyond tree level. This evolution is typically negligible for light quarks because of the m^4 factor.

APPENDIX C: $\overline{\text{MS}}$ CONDENSATES FROM THE LATTICE

The coefficient functions in operator-product expansions such as Eq. (B3) are most conveniently computed using the $\overline{\text{MS}}$ regulator to define the operators on the right-hand side. On the other hand, the only technology available for determining the nonperturbative matrix elements needed in such analyses is lattice simulation, using the lattice ultraviolet regulator. To combine these techniques we must be able to convert lattice determinations of $\langle 0|m\bar{\psi}\psi|0\rangle$, for example, into the equivalent $\overline{\text{MS}}$ matrix elements.

The relationship is again given by the operator product expansion:

$$(m\bar{\psi}\psi)^{(\mu)}_{\overline{\text{MS}}} = \mathbf{1}^{(a)}\frac{m^2}{a^2}f(\mu \leftrightarrow \pi/a)$$
$$+ (m\bar{\psi}\psi)^{(a)}_{\text{LQCD}}h(\mu \leftrightarrow \pi/a) + \cdots, \quad \text{(C1)}$$

where the coefficient functions f and h can only depend upon physics between μ and the lattice cutoff π/a. In fact $h = 1$ since the matrix elements in

$$h = \frac{\langle q|m\bar{\psi}\psi|q'\rangle^{(\mu)}_{\overline{\text{MS}}}}{\langle q|m\bar{\psi}\psi|q'\rangle^{(a)}_{\text{LQCD}}} = 1 \quad \text{(C2)}$$

are μ and a independent, and therefore h must be a number (and 1 is the correct number, from perturbation theory). The coefficient function f is computed order by order in perturbation theory using the expansions of the two condensates (computed with their respective regulators):

$$f \equiv \frac{a^2}{m^2}(\langle 0|m\bar{\psi}\psi|0\rangle^{(\mu)}_{\overline{\text{MS}}} - \langle 0|m\bar{\psi}\psi|0\rangle^{(a)}_{\text{LQCD}})_{\text{PQCD}}$$
$$= \sum_{n=0} f_n^{(0)}(a\mu)\alpha_{\overline{\text{MS}}}^n(\mu) + (am)^2\sum_{n=0} f_n^{(1)}(a\mu)\alpha_{\overline{\text{MS}}}^n(\mu). \quad \text{(C3)}$$

The cancellation of all $\log m$ terms between the two matrix elements in f is something of a miracle; it only works if the m in each case is precisely the m that multiplies $\bar{\psi}\psi$ in the action for that case.[3] Δ_{PT} in Eq. (21) is $(am)^2f$ calculated through $\mathcal{O}(\alpha_s)$.

Additional terms appear in Eq. (C1) from mixing with higher dimension condensates, such as the gluon condensate. These are suppressed by positive powers of a. For the gluon condensate the multiplier is $(ma)^2$ from chirality arguments. These terms then simply look like discretization errors in $m\bar{\psi}\psi$ and are handled as part of the general treatment of those errors.

APPENDIX D: LATTICE QCD CALCULATION ON $n_f = 2 + 1$ GLUON CONFIGURATIONS

We show here further results for the strange quark condensate from two contrasting calculations, both using HISQ quarks, that include u, d and s quarks in the sea, but no c quarks. The first calculation uses sets of MILC configurations corresponding to five values of lattice spacing spanning a large range from 0.15 to 0.04 fm [26] and using the asqtad formalism for the sea quarks. The second uses HOTQCD configurations [36] and has more lattice spacing values (24 in total) but with only a limited number (9) having accompanying meson masses and decay constants. The sea quarks are included using the HISQ formalism with u/d sea quark masses close to the physical value. The second calculation corresponds to the zero temperature results generated to accompany a finite temperature analysis of the phase structure of QCD. This analysis needs

---

[3]If this is not the case, then the coefficient function h will not equal 1, but rather will be a series in $\alpha_{\overline{\text{MS}}}$.

TABLE VI.   Raw (unsubtracted) values for the strange quark condensate along with η_s masses and decay constants in lattice units calculated for valence masses given in column 4. The calculations use valence HISQ quarks on MILC configuration sets labeled in column 1 that include $2 + 1$ flavors of asqtad quarks (see Ref. [26] for more details about the ensembles). The results are derived from the correlators calculated in Refs. [26,49] along with Eq. (11), but also give results for additional strange quark masses on sets 1 and 2. δx_{sea} is the mismatch between the sea $2m_l + m_s$ value and the physical result divided by the physical value of m_s [49].

Set	δx_{sea}	a_{η_s} (fm)	$am_{s,\text{val}}$	aM_{η_s}	af_{η_s}	$-a^3\langle\bar{\psi}\psi_s\rangle_0$
1	0.47	0.1583(13)	0.061	0.50490(36)	0.1410(4)	0.042399(38)
			0.066	0.52524(36)	0.1429(4)	0.044637(38)
			0.080	0.57828(34)	0.1485(4)	0.050795(37)
2	0.91	0.1595(14)	0.066	0.52458(35)	0.1434(3)	0.044714(37)
3	0.64	0.1247(10)	0.0489	0.41133(17)	0.1124(2)	0.030233(14)
			0.0537	0.4310(4)	0.1144(2)	0.032423(15)
4	0.93	0.1264(11)	0.0492	0.41436(23)	0.1136(2)	0.030585(21)
			0.0546	0.43654(24)	0.1160(3)	0.033041(20)
			0.060	0.45787(23)	0.1182(4)	0.035476(20)
5	1.5	0.1263(11)	0.0491	0.41196(24)	0.1135(2)	0.030306(21)
			0.0525	0.4259(6)	0.1149(4)	0.031817(23)
			0.0556	0.4384(6)	0.1161(4)	0.033211(23)
6	0.59	0.0878(7)	0.0337	0.29413(12)	0.07954(9)	0.018310(5)
			0.0358	0.30332(12)	0.08051(9)	0.019273(5)
			0.0382	0.31362(14)	0.08171(15)	0.020370(5)
7	1.1	0.0884(7)	0.0336	0.29309(13)	0.07959(11)	0.018217(5)
			0.03635	0.30513(20)	0.08095(14)	0.019467(7)
8	0.28	0.0601(5)	0.0228	0.20621(19)	0.0549(2)	0.011311(5)
			0.024	0.21196(13)	0.0556(1)	0.011851(3)
9	0.38	0.0443(4)	0.0161	0.1525(2)	0.0404(1)	0.0075891(20)

many values of the lattice spacing for a fine-grained temperature scale, and the zero temperature results are needed to fix the QCD parameters. The quark condensate is an important order parameter at finite temperature but is also determined in Ref. [36] on the zero temperature ensembles.

For the first calculation we use values of the strange quark condensate listed in Table VI. These are obtained from studies of the η_s correlator on nine different ensembles at five different values of the lattice spacing and multiple sea quark mass values. The lattice spacing values we use here are defined from the η_s decay constant and are determined in Ref. [26]. From the values in Table VI we can construct the ratio R_s defined in Eq. (24) and fit it as a function of lattice spacing in exactly the same way as that described in Sec. III B 2. The $\mathcal{O}(\alpha_s^0)$ and $\mathcal{O}(\alpha_s^1)$ perturbative subtractions defined in Sec. III A apply here also since no effects appear at this order from the differing number of sea quarks or the formalism used for them, or the improvement coefficients in the gluon action (the MILC $2 + 1$ asqtad configurations do not include the $n_f\alpha_s a^2$ improvement coefficients in the gluon action). These effects will cause differences in the perturbation theory at $\mathcal{O}(\alpha_s^2)$. The α_s^2 and higher order divergent pieces of the condensate are included in the fit with coefficients that, as before, are given a prior value of 0(4). The appropriate α_s value in this case is $\alpha_V^{n_f=3}(2/a)$ rather than $\alpha_V^{n_f=4}(2/a)$. Multiple valence s quark masses are given at each lattice spacing

and we allow for linear and quadratic dependence on the mistuning of the s quark mass, again as described in Sec. III B 2. We allow for mistuning of the sea quark masses through use of the parameter δx_{sea} [49].

Figure 12 shows, as a hatched band, the physical result from the fit, which has $\chi^2/\text{d.o.f.} = 0.4$ for 20 degrees of freedom. For comparison the data points given are the values after perturbative subtraction through $\mathcal{O}(\alpha_s)$. The physical value obtained is

$$R_{s,\text{phys}} = 0.555(84). \tag{D1}$$

This is completely consistent with the result from $2 + 1 + 1$ flavors of HISQ sea quarks in Sec. III B 2, and has a similar error. It is not such a complete calculation, lacking light quark mass results and not having such light sea quark masses, and is therefore not our preferred final result. It provides a strong check of our $2 + 1 + 1$ result, however, being a completely independent set of numbers. The fits to the $2 + 1$ results give very similar behavior to that seen for the $2 + 1 + 1$ case, for example choosing a coefficient of the α_s^2/a^2 divergence of around 2.

For the second calculation we use values of the strange condensate from the HOTQCD collaboration [36]. They generated ensembles with an improved gluon action and u/d and s quarks in the sea using the HISQ formalism. The QCD action differs slightly from that in Sec. III. Apart from missing c quarks in the sea, the gauge field
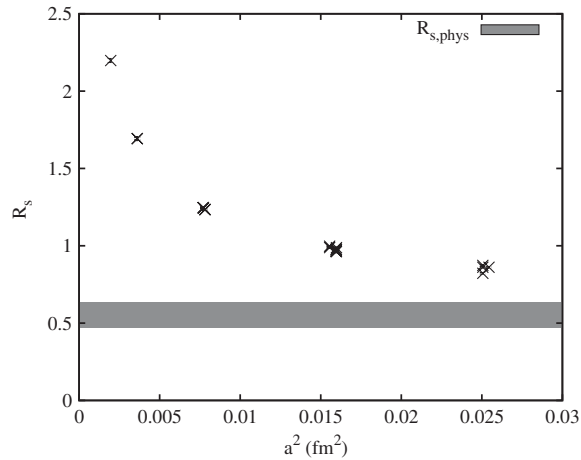
FIG. 12. Results from fitting the values for R_s obtained on MILC configurations including $2 + 1$ flavors of asqtad sea quarks, as described in the text. The crosses give the calculated values after perturbative subtraction through $\mathcal{O}(\alpha_s)$. The hatched band corresponds to the fitted physical value after removing the remaining power divergence and discretization and sea quark mass effects. Compare to Fig. 6 which includes $2 + 1 + 1$ flavors of HISQ sea quarks.

configurations here are improved through $\mathcal{O}(a^2)$ at tree level and without tadpole improvement, i.e., the fairly substantial $\mathcal{O}(\alpha_s a^2)$ improvement coefficients were not included. The lattice spacing was determined using the r_1 heavy quark potential parameter, or r_0 on the coarsest lattices where $r_1/a < 2$. The s quark mass was tuned by determining the mass of the η_s meson and the light quark mass was taken as $m_s/20$ (with some values available for $m_s/5$ but we have not used those). Results for the zero temperature strange condensate are available at 24 values of the lattice spacing from 0.2 to 0.07 fm (Table 14 of Ref. [36] gives values for two times the condensate). Note that these results were obtained by direct calculation of $\langle \mathrm{Tr} M^{-1} \rangle$ using stochastic techniques. Corresponding values of the lattice spacing are given in Table 16 of Ref. [36]; some missing values can be inferred from the tables of temperature values at the corresponding value of β.

Figure 13 shows the raw unsubtracted results for $m_s \langle \bar{\psi} \psi_s \rangle$ as a function of the square of the inverse lattice spacing, as well as the values after making the complete subtraction through $\mathcal{O}(\alpha_s)$ as given in Eq. (21). As for R_s in Sec. III B 1 (Fig. 4), the unsubtracted results show clear evidence of a quadratic term in a^{-1} which is significantly
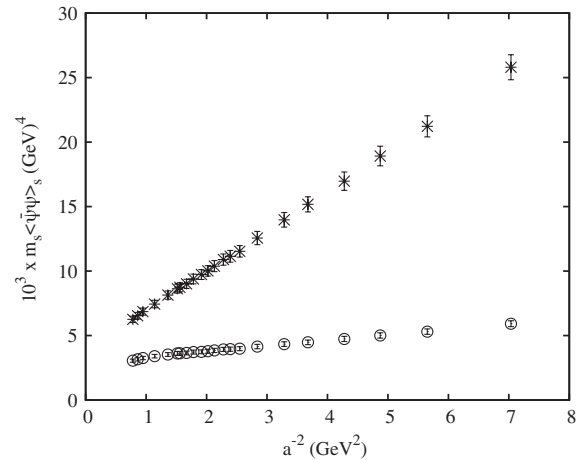

FIG. 13. Bursts give the raw data for $m_s \langle \bar{\psi} \psi_s \rangle$ from Ref. [36] as a function of the square of the inverse lattice spacing. Open circles give results after subtraction of the $\mathcal{O}(\alpha_s)$ perturbative contribution.

reduced, but not completely absent, after the perturbative subtraction.

For a subset of nine lattice spacing values meson masses and decay constants are also given in Tables 18 and 19 of Ref. [36]. In fact we use the seven finest values only because the s quark mass is not as well tuned for our purposes on the coarsest two lattices. Note that the decay constant values need to be multiplied by $\sqrt{2}$ to match the convention used here. For these we can construct the ratio R_s given in (24). To obtain a physical result for R_s we fit the subtracted results as a function of lattice spacing in the same way as in Sec. III B 2, apart from the use of $\alpha_V^{n_f=3}(2/a)$ rather than $\alpha_V^{n_f=4}(2/a)$.

The physical value for R_s obtained from the fit is

$$R_s = 0.79(34). \qquad (\text{D2})$$

This is much less accurate than the result from Sec. III, but agrees both with that and the result from the MILC $2 + 1$ asqtad ensembles given earlier in this section. We have not extracted a light quark condensate from the HOTQCD results because finite volume sensitivity obscures the power divergence and leads to larger errors.

We conclude from this that there is no sign of disagreement between the strange quark condensate extracted with u, d and s quarks in the sea and those including also c quarks in the sea.

[1] L. Reinders, H. Rubinstein, and S. Yazaki, Phys. Rep. **127,** 1 (1985).

[2] M. Gell-Mann, R. Oakes, and B. Renner, Phys. Rev. **175,** 2195 (1968).

[3] S. Borsanyi, S. Durr, Z. Fodor, S. Krieg, A. Schafer *et al.*, arXiv:1205.0788.

[4] M. A. Shifman, A. Vainshtein, and V. I. Zakharov, Nucl. Phys. **B147,** 448 (1979).

[5] M. A. Shifman, Prog. Theor. Phys. Suppl. **131**, 1 (1998).

[6] K. Chetyrkin, V. Spiridonov, and S. Gorishnii, Phys. Lett. **160B**, 149 (1985).

[7] M. Jamin and M. Munz, Z. Phys. C **60**, 569 (1993).

[8] J. Koponen *et al.* (HPQCD), Proc. Sci. LATTICE (2010) 231 [arXiv:1011.1208].

[9] E. Shintani, S. Aoki, H. Fukaya, S. Hashimoto, T. Kaneko, T. Onogi, and N. Yamada, Phys. Rev. D **82**, 074505 (2010).

[10] E. Gamiz, M. Jamin, A. Pich, J. Prades, and F. Schwab, J. High Energy Phys. 01 (2003) 060.

[11] R. Albuquerque, S. Narison, and M. Nielsen, Phys. Lett. B **684**, 236 (2010).

[12] K. Maltman, Phys. Lett. B **672**, 257 (2009).

[13] E. Follana, Q. Mason, C. Davies, K. Hornbostel, G. P. Lepage, J. Shigemitsu, H. Trottier, and K. Wong (HPQCD), Phys. Rev. D **75**, 054502 (2007).

[14] T. Banks and A. Casher, Nucl. Phys. **B169**, 103 (1980).

[15] H. Leutwyler and A. Smilga, Phys. Rev. D **46**, 5607 (1992).

[16] E. V. Shuryak and J. Verbaarschot, Nucl. Phys. **A560**, 306 (1993).

[17] P. Damgaard, Nucl. Phys. B, Proc. Suppl. **106–107**, 29 (2002).

[18] E. Follana, A. Hart, C. T. H. Davies, and Q. Mason (HPQCD), Phys. Rev. D **72**, 054501 (2005).

[19] E. Braaten, S. Narison, and A. Pich, Nucl. Phys. **B373**, 581 (1992).

[20] P. Hernandez, K. Jansen, and L. Lellouch, Phys. Lett. B **469**, 198 (1999).

[21] F. David and H. W. Hamber, Nucl. Phys. **B248**, 381 (1984).

[22] C. T. H. Davies, K. Hornbostel, I. D. Kendall, G. P. Lepage, C. McNeile, J. Shigemitsu, and H. Trottier (HPQCD), Phys. Rev. D **78**, 114507 (2008).

[23] R. J. Dowdall, B. Colquhoun, J. Daldrop *et al.* (HPQCD), Phys. Rev. D **85**, 054509 (2012).

[24] A. Bazavov *et al.* (MILC), Phys. Rev. D **82**, 074501 (2010).

[25] A. Hart, G. M. von Hippel, and R. R. Horgan (HPQCD), Phys. Rev. D **79**, 074008 (2009).

[26] C. Davies, E. Follana, I. Kendall, G. Lepage, and C. McNeile (HPQCD), Phys. Rev. D **81**, 034506 (2010).

[27] G. W. Kilcup and S. R. Sharpe, Nucl. Phys. **B283**, 493 (1987).

[28] J. Gasser and H. Leutwyler, Nucl. Phys. **B250**, 465 (1985).

[29] M. Jamin, Phys. Lett. B **538**, 71 (2002).

[30] D. Toussaint (private communication).

[31] C. McNeile, C. Davies, E. Follana, K. Hornbostel, and G. Lepage (HPQCD), Phys. Rev. D **82**, 034512 (2010).

[32] G. P. Lepage, B. Clark, C. T. H. Davies, K. Hornbostel, P. B. Mackenzie, C. Morningstar, and H. Trottier, Nucl. Phys. B, Proc. Suppl. **106–107**, 12 (2002).

[33] A. Bazavov, D. Toussaint, C. Bernard, J. Laiho, C. DeTar *et al.*, Rev. Mod. Phys. **82**, 1349 (2010).

[34] C. T. H. Davies, C. McNeile, K. Y. Wong, E. Follana, R. Horgan, K. Hornbostel, G. P. Lepage, J. Shigemitsu, and H. Trottier (HPQCD), Phys. Rev. Lett. **104**, 132003 (2010).

[35] A. Bazavov *et al.* (MILC), Proc. Sci. LATTICE (2009) 079 [arXiv:0910.3618].

[36] A. Bazavov, T. Bhattacharya, M. Cheng, C. DeTar, H. Ding *et al.* (HotQCD), Phys. Rev. D **85**, 054503 (2012).

[37] S. Narison, arXiv:hep-ph/0202200.

[38] C. A. Dominguez, N. F. Nasrallah, R. Rontsch, and K. Schilcher, J. High Energy Phys. 05 (2008) 020.

[39] A. Gray, M. Wingate, C. T. H Davies, E. Gulez, G. P. Lepage, Q. Mason, M. Nobes, and J. Shigemitsu (HPQCD), Phys. Rev. Lett. **95**, 212001 (2005).

[40] C. Bernard *et al.* (Fermilab Lattice, MILC, and HPQCD), Proc. Sci. LAT (2007) 370.

[41] C. Davies, Proc. Sci. LATTICE (2011) 019 [arXiv:1203.3862].

[42] J. Bordes, C. Dominguez, P. Moodley, J. Penarrocha, and K. Schilcher, J. High Energy Phys. 05 (2010) 064.

[43] H. Fukaya, S. Aoki, T. W. Chiu, S. Hashimoto, T. Kaneko, J. Noaki, T. Onogi, and N. Yamada (JLQCD and TWQCD), Phys. Rev. D **83**, 074501 (2011).

[44] F. Burger, V. Lubicz, M. Muller-Preussker, S. Simula, and C. Urbach, arXiv:1210.0838.

[45] G. Colangelo, S. Durr, A. Juttner, L. Lellouch, H. Leutwyler *et al.*, Eur. Phys. J. C **71**, 1695 (2011).

[46] S. J. Brodsky, C. D. Roberts, R. Shrock, and P. C. Tandy, Phys. Rev. C **82**, 022201 (2010).

[47] R. Frezzotti, G. Martinelli, M. Papinutto, and G. Rossi, J. High Energy Phys. 04 (2006) 038.

[48] I. Allison, E. Dalgic, C. Davies *et al.*, Phys. Rev. D **78**, 054513 (2008).

[49] C. T. H. Davies, C. McNeile, E. Follana, G. P. Lepage, H. Na, and J. Shigemitsu (HPQCD), Phys. Rev. D **82**, 114504 (2010).